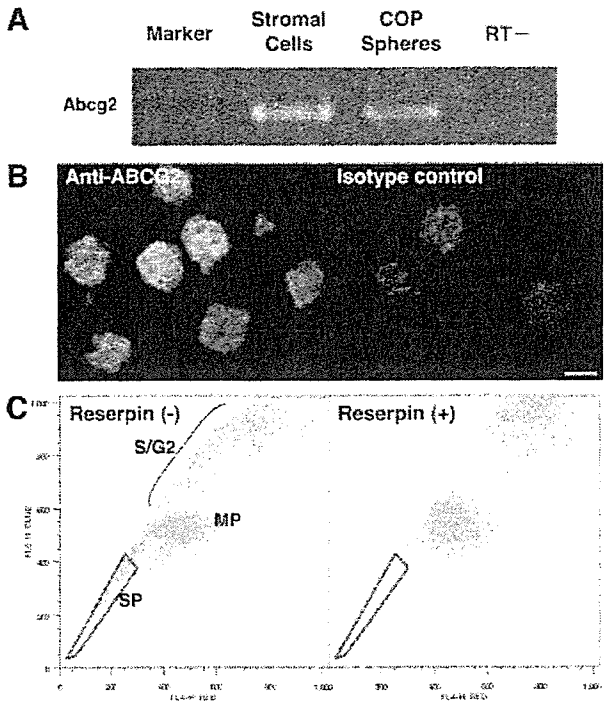

Figure 4. Murine COPs show ABCG2 expression and the SP cell phenotype. (**A**): RT-polymerase chain reaction analysis revealed *Abcg2* expression in COP spheres and in cells freshly dissociated from mouse corneal stroma. (**B**): Immunofluorescent staining of ABCG2 in COP spheres. Nuclei were counterstained with 4,6-diamidino-2-phenylindole. Scale bar = 100 μm. (**C**): Approximately 3.3% of sphere cells were SP cells as shown by flow cytometry. Hypofluorescent SP cells are distinct from MP cells and disappear when treated with reserpine, an inhibitor of ABCG2. Cells in the S/G_2 phase were not gated as SP cells, even though they disappeared with reserpine treatment. Abbreviations: COP, cornea-derived precursor; MP, main population; RT, reverse transcription; SP, side population.

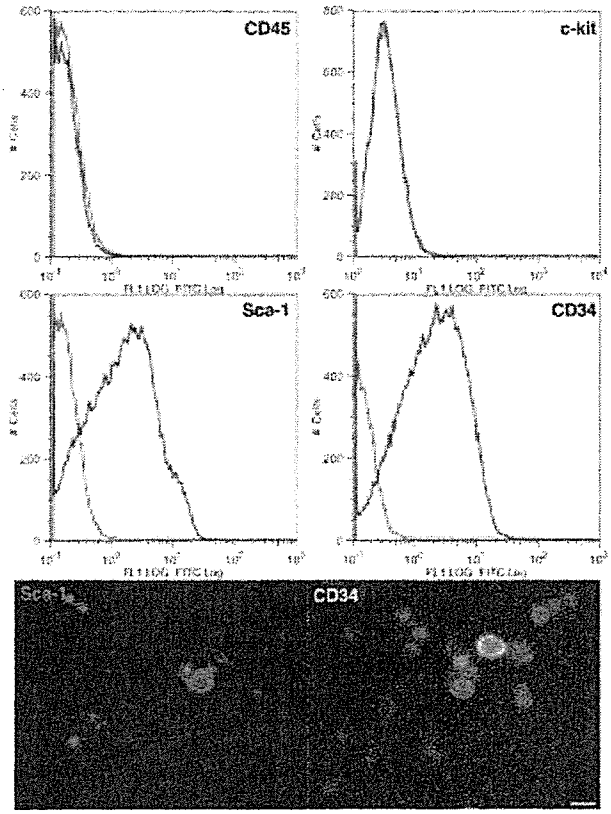

Figure 5. Cornea-derived precursors (COPs) express stem cell surface markers. (**A**): Single cells dissociated from COP spheres were stained with antibodies for CD45, c-kit, Sca-1, or CD34 and analyzed by flow cytometry (blue lines). Red lines represent isotype-matched negative control. COP sphere cells did not express CD45 or c-kit but did express Sca-1 and CD34. (**B**): Fluorescent images of cells stained with phycoerythrin-labeled anti-Sca-1 (left, red) or FITC-labeled anti-CD34 (right, green). Scale bar = 20 μm. Abbreviation: FITC, fluorescein isothiocyanate.

4A, 4B). Reserpine-sensitive SP cells were detected in dissociated sphere cells, representing 3.3% ± 1.2% (n = 8) of viable cells analyzed by flow cytometry (Fig. 4C).

We also analyzed several stem cell-related surface markers by flow cytometry. COP spheres expressed CD34 (Fig. 5A, 5B), a cell surface marker reported in rodent epithelial stem cells in the bulge area [35, 36], skeletal muscle stem cells [37, 38], and corneal stromal cells [9, 39]. In addition, expression of stem cell antigen-1 (Sca-1), a cell surface protein expressed in BM-derived hematopoietic stem cells (BM-HSCs) [40], mammary epithelial stem cells [41], a subpopulation of BM stromal cells [42], skeletal muscle stem cells [38], and SKP spheres [12], was found in 56.1% ± 19.2% (n = 7) of viable cells (Fig. 5). The expression of CD133, found in different types of primitive cells such as BM-HSCs, NSCs, and SKPs [43–46], was not observed (data not shown). Another cell surface marker, c-kit (CD117), the receptor for stem cell factor and a marker of BM-HSCs [47], was also not detected by flow cytometric analysis (Fig. 5) and RT-PCR (not shown).

COPs Are Neural Crest Lineage Cells

Although we found $CD34^+$ cells in COP spheres, Sosnova et al. [48] reported that all $CD34^+$ cells in mouse corneal stroma are $CD45^+$ BM-derived cells. In addition, the ability of BM-derived mesenchymal stem cells (BM-MSCs) to differentiate into multiple cell types has been reported [49, 50]. However, we found that COPs did not express CD45 (0.2% ± 0.2%, n = 6; Fig. 5A), indicating a nonhematopoietic origin for these cells. We further prepared COPs from mice transplanted with GFP^+ WBM cells. GFP^+ cells were not found in COP spheres prepared from the recipient mice 8 weeks after transplantation (Fig. 6C), although numerous GFP^+ cells were observed in the recipient cornea (Fig. 6A, 6B). GFP^+ cells in sphere culture preparations were found attached to the bottom of the culture dish, and immunofluorescent staining showed that the GFP^+ cells were $CD45^+$ and some also expressed CD34 (Fig. 6D). CD34 was therefore expressed in both BM-derived GFP^+ cells as well as GFP-COPs, indicating that WBM-derived cells are not likely to contribute to COP sphere-initiating cells.

Given that cranial neural crest-derived mesenchymal cells contribute to corneal stroma development, we next investigated whether COPs were of neural crest origin [6, 7]. COP spheres were prepared from Wnt1-Cre/Floxed-EGFP and P0-Cre/Floxed-EGFP transgenic mice in which neural crest-derived cells are tagged by EGFP expression [14, 51]. As expected, COP spheres prepared

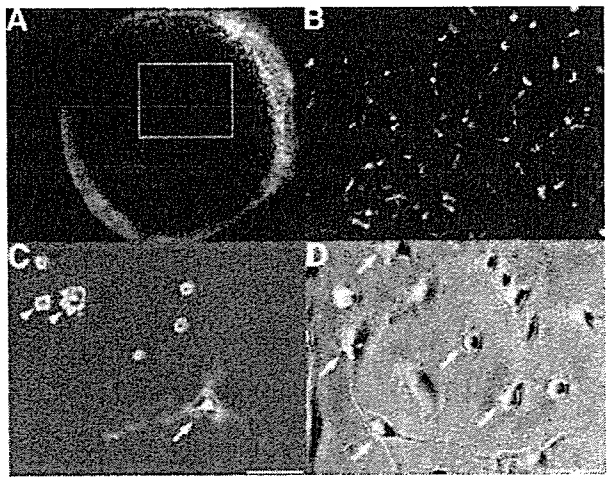

Figure 6. Bone marrow cells do not form cornea-derived precursor (COP) spheres. Sphere cultures prepared from C57BL6/J mice transplanted with whole bone marrow (WBM) cells of green fluorescent protein (GFP) mice did not produce GFP^+ spheres. **(A):** Fluorescent image of a cornea 8 weeks after WBM cell transplantation. Migration of numerous GFP^+ cells into the cornea was observed. **(B):** High-magnification view of the boxed area in **(A)**. **(C):** Phase-contrast image merged with fluorescent image of sphere culture at 7 days after plating. GFP^+ WBM-derived cells were found attached to the culture dish (arrow), whereas GFP^+ cells were not observed in forming spheres (arrowhead). **(D):** Adherent cells were stained with phycoerythrin-labeled anti-CD34 antibody (red). CD34 (arrows) was also expressed in transplanted WBM-derived cells (green). Scale bars = 200 μm **(C, D)**.

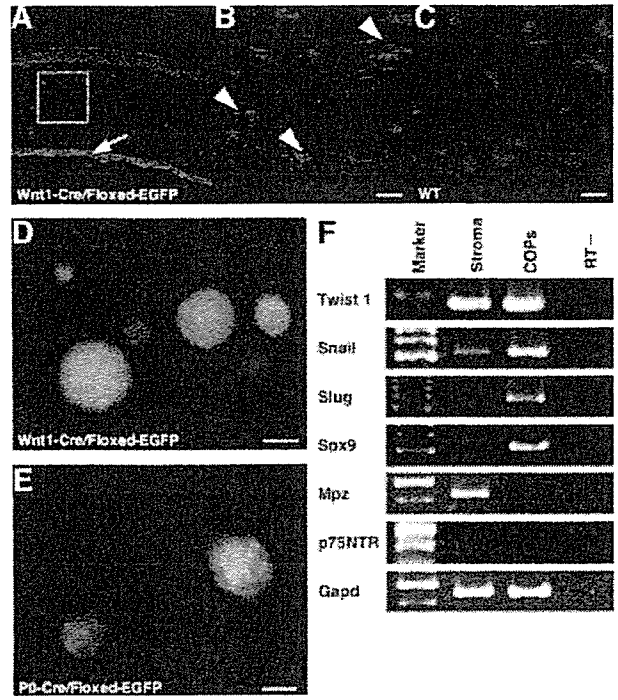

Figure 7. COPs are neural crest-derived cells. **(A–C):** Confocal images of Wnt1-Cre/Floxed-EGFP mouse **(A, B)** and WT mouse cornea **(C)** stained with anti-GFP antibody and cyanine 3-conjugated secondary antibody. **(B):** High-magnification view of the boxed region in **(A)**. Expression of EGFP is detected in keratocytes, although the expression level is low in vivo **(B)** (arrowheads). Positive staining is also detected in corneal endothelium, which is also neural crest-derived **(A)** (arrow). Cells dissociated from corneal stroma of Wnt1-Cre/Floxed-EGFP **(D)** (day 14) and P0-Cre/Floxed-EGFP mice **(E)** (day 6) formed $EGFP^+$ COP spheres. **(F):** Expression of embryonic neural crest markers by COPs and corneal stromal tissue. *Gapd* was loaded as an internal control. Expression of *Snail*, *Slug*, and *Sox9* was upregulated in COP spheres, whereas *Twist* was found in both COPs and stroma. *Mpz* was detected from stromal tissue only. Scale bars = 50 μm **(A, D, E)** and 20 μm **(B, C)**. Abbreviations: COP, cornea-derived precursor; EGFP, enhanced green fluorescent protein; GFP, green fluorescent protein; RT, reverse transcription; WT, wild-type.

from both transgenic mice were GFP^+ (Fig. 7D, 7E). To visualize GFP^+ neural crest-derived cells in the cornea, sections of Wnt1-Cre/Floxed-EGFP mouse were immunostained using anti-GFP antibody. Expression of GFP was detected in stromal keratocytes, although the expression level was low in vivo (Fig. 7B). Strong immunoreactivity was detected in the corneal endothelium (Fig. 7A), which are also neural crest-derived [52, 53]. We also examined embryonic neural crest-associated genes by RT-PCR analysis. *Twist*, *Slug*, *Snail*, and *Sox9* were expressed in COPs (Fig. 7F). These data confirm that COPs are neural crest-derived stem cells that are not recruited from the BM.

Discussion

The expansion of stem cells in vitro while maintaining properties of progenitor cells is critical from the standpoint of using stem cells for research as well as medical purposes. Culture conditions for several adult somatic stem cells, including BM-HSCs and NSCs, have been well-established. The sphere culture technique, which was originally developed for culturing NSCs as neurosphere from the central nervous system (CNS), was recently applied to isolate sphere-initiating cells from adult tissues other than CNS [2, 10–12, 17, 51, 54]. COPs have been subcultured for more than 13 months (more than 18 passages, corresponding to more than 90 population doublings) to date. As we discovered, not only do these cells have the ability to differentiate into keratocytes, fibroblasts, and myofibroblasts as observed in primary stromal keratocytes [9], COPs can also be induced to differentiate into adipocytes, chondrocytes, and neural cells.

Clonal spheres in this study were initiated using methylcellulose, which is an established method to clone hematopoietic cells and, more recently, embryonic stem cells and NCSs [17–24]. Cells within a sphere arising from a single cell were not necessarily homogeneous, which may be due to the position within a sphere or to autocrine and paracrine mechanisms. Dark cells in spheres (Fig. 1) were not GFP-negative but simply had low fluorescence under the conditions of our photography, which were set with exposure settings that do not cause saturation of fluorescent levels. This is vital because long exposure times can give the misleading impression of strong fluorescence in 100% of the cells, which is not the case.

We have also demonstrated that COPs include a high ratio of SP cells with Hoechst dye exclusion activity, which are regarded as a general property of progenitor-candidate cells. Although a higher percentage of cells seem to be ABCG2-positive by immunocytochemical analysis compared with flow cytometry, not all ABCG2-positive cells are drawn into the SP gate, which was defined by the inhibition of functional ABC transporters. Indeed, reserpine-sensi-

tive SP-like cells were found outside the SP gate, which may have been dividing cells exhibiting higher fluorescent intensity. The results of ABCG2 expression in COPs and the high fraction of SP cells suggest that the Hoechst dye exclusion assay may be used to further characterize COPs. A recent study by Du et al. also demonstrated the presence of SP cells in the human peripheral corneal stroma, which were shown to express neural and cartilage markers in addition to keratocyte markers [55]. We have confirmed that COP SP cells re-formed spheres after cell sorting (data not shown).

Other stem cell-related markers, including *nestin*, *Notch1*, and *Msi1*, were also expressed in COP spheres. Although the upregulation of Nestin is often used as evidence of a NSC phenotype, expression of this intermediate filament protein in non-neuronal cells has also been reported [56]. We therefore prepared COP spheres from transgenic mice carrying EGFP under the control of a neural-selective enhancer of the *nestin* gene [57–59]. Given that no fluorescence was observed in corneas of these mice, expression of nestin in corneal stromal cells revealed by RT-PCR analysis is probably due to non-neuronal expression. However, the fluorescence observed in COPs prepared from E/nestin-EGFP transgenic mice suggests that the neural stem/progenitor cell-specific enhancer was activated. Interestingly, we also found that expression of *Msi1* was upregulated only in COPs but not in the corneal stroma of the original mice. Recent reports demonstrated that Msi1 is expressed by epithelial stem cells in intestine [60, 61] and mammary gland [62], making Msi1 a candidate marker of adult stem cells in a variety of tissue sources.

There are only a limited number of reports describing putative progenitor cells for corneal keratocytes [2, 3]. Stromal keratocytes develop from mesenchymal cells originating in the cranial neural crest [6, 7]. A recent study demonstrated that late embryonic keratocytes maintain plasticity to differentiate into other neural crest-derived tissue when transplanted into embryos [63]. On the other hand, several reports have shown that BM-derived cells migrate to the corneal stroma [64, 65]. Recently, Sosnova et al. [48] reported that keratocytes do not express CD34 in the mouse corneal stroma and that all $CD34^+$ cells coexpressed CD45 and were therefore BM-derived. However, Espana et al. [39] reported CD34 expression in cultured human keratocytes. We found $CD34^+CD45^-$ cells in COP spheres (Fig. 5), which were distinct from the $CD34^+CD45^+$ adhesive cells isolated from corneas of GFP^+ WBM transplanted mice (Fig. 6). Given that GFP^+ COP spheres were not observed in GFP^+ WBM transplanted mice, COPs appear to be non-BM progenitors that express CD34, at least during sphere cultures. Furthermore, COPs prepared from Wnt1-Cre/Floxed-EGFP and P0-Cre/Floxed-EGFP mice were $EGFP^+$ (Fig. 7), strongly suggesting that these cells prepared from the cornea are of neural crest origin. Anti-GFP immunostaining also revealed neural crest-derived cells in the corneal stroma of Wnt1-Cre/Floxed-EGFP mice, with weaker levels of GFP expression in the stroma (Fig. 7B) compared with the endothelium (Fig. 7A). The weak expression of GFP in the stroma is probably due to the thin dendritic morphology of keratocytes, as well as the fact that stromal keratocytes are quiescent in vivo [66–68].

Further investigations are required to determine whether COPs are unique cells that reside in the corneal stroma or whether they represent a lineage of NSCs common with SKPs that migrate to the cornea. Although there is still controversy as to the identity of SKPs [69], the similarity of COPs with SKPs also has several clinical implications for the possible use of dermal cells for reconstructing the corneal stroma. If abundant dermal SKPs can be induced to differentiate into keratocytes, the development of corneal equivalents using autologous tissue may become a reality. Further studies to isolate COPs from humans for regenerative purposes are under way.

ACKNOWLEDGMENTS

We thank Kimie Kato for technical assistance, Hiroko Kouike for expert assistance with flow cytometric analysis, Fumito Morito for cell cultures, and Prof. Masaru Okabe (Genome Information Research Center) for providing the GFP-transgenic mice (C57BL/6 TgN [act-EGFP]OsbC14-Y01-FM131). This study was partly supported by a grant from the Advanced and Innovational Research Program in Life Sciences from the Ministry of Education, Culture, Sports, Science and Technology of Japan (to T.K. and H.O.), a grant from Core Research for Evolutional Science and Technology (CREST) of Japan Science and Technology Corporation (to H.O.), and a grant-in-aid to Keio University from the 21st Century Center of Excellence (COE) program.

DISCLOSURES

The authors indicate no potential conflicts of interest.

REFERENCES

1 Lavker RM, Tseng SC, Sun TT. Corneal epithelial stem cells at the limbus: Looking at some old problems from a new angle. Exp Eye Res 2004;78:433–446.

2 Uchida S, Yokoo S, Yanagi Y et al. Sphere formation and expression of neural proteins by human corneal stromal cells in vitro. Invest Ophthalmol Vis Sci 2005;46:1620–1625.

3 Funderburgh ML, Du Y, Mann MM et al. PAX6 expression identifies progenitor cells for corneal keratocytes. FASEB J 2005;19: 1371–1373.

4 Wilson SE, Pedroza L, Beuerman R et al. Herpes simplex virus type-1 infection of corneal epithelial cells induces apoptosis of the underlying keratocytes. Exp Eye Res 1997;64:775–779.

5 Helena MC, Baerveldt F, Kim WJ et al. Keratocyte apoptosis after corneal surgery. Invest Ophthalmol Vis Sci 1998;39:276–283.

6 Johnston MC, Noden DM, Hazelton RD et al. Origins of avian ocular and periocular tissues. Exp Eye Res 1979;29:27–43.

7 Trainor PA, Tam PP. Cranial paraxial mesoderm and neural crest cells of the mouse embryo: Co-distribution in the craniofacial mesenchyme but distinct segregation in branchial arches. Development 1995;121: 2569–2582.

8 Reynolds BA, Weiss S. Generation of neurons and astrocytes from isolated cells of the adult mammalian central nervous system. Science 1992;255:1707–1710.

9 Yoshida S, Shimmura S, Shimazaki J et al. Serum-free spheroid culture of mouse corneal keratocytes. Invest Ophthalmol Vis Sci 2005;46: 1653–1658.

10 Toma JG, McKenzie IA, Bagli D et al. Isolation and characterization of multipotent skin-derived precursors from human skin. STEM CELLS 2005;23:727–737.

11 Toma JG, Akhavan M, Fernandes KJ et al. Isolation of multipotent adult stem cells from the dermis of mammalian skin. Nat Cell Biol 2001;3: 778–784.

12 Fernandes KJ, McKenzie IA, Mill P et al. A dermal niche for multipotent adult skin-derived precursor cells. Nat Cell Biol 2004;6:1082–1093.

13 Danielian PS, Muccino D, Rowitch DH et al. Modification of gene activity in mouse embryos in utero by a tamoxifen-inducible form of Cre recombinase. Curr Biol 1998;8:1323–1326.

14 Yamauchi Y, Abe K, Mantani A et al. A novel transgenic technique that allows specific marking of the neural crest cell lineage in mice. Dev Biol 1999;212:191–203.

15 Kawamoto S, Niwa H, Tashiro F et al. A novel reporter mouse strain that expresses enhanced green fluorescent protein upon Cre-mediated recombination. FEBS Lett 2000;470:263–268.

16 Okabe M, Ikawa M, Kominami K et al. 'Green mice' as a source of ubiquitous green cells. FEBS Lett 1997;407:313–319.

17 Kawase Y, Yanagi Y, Takato T et al. Characterization of multipotent adult stem cells from the skin: Transforming growth factor-beta (TGF-beta) facilitates cell growth. Exp Cell Res 2004;295:194–203.

18 Suslov ON, Kukekov VG, Ignatova TN et al. Neural stem cell heterogeneity demonstrated by molecular phenotyping of clonal neurospheres. Proc Natl Acad Sci U S A 2002;99:14506–14511.

19 Ignatova TN, Kukekov VG, Laywell ED et al. Human cortical glial tumors contain neural stem-like cells expressing astroglial and neuronal markers in vitro. Glia 2002;39:193–206.

20 Laywell ED, Rakic P, Kukekov VG et al. Identification of a multipotent astrocytic stem cell in the immature and adult mouse brain. Proc Natl Acad Sci U S A 2000;97:13883–13888.

21 Kukekov VG, Laywell ED, Suslov O et al. Multipotent stem/progenitor cells with similar properties arise from two neurogenic regions of adult human brain. Exp Neurol 1999;156:333–344.

22 Gritti A, Frolichsthal-Schoeller P, Galli R et al. Epidermal and fibroblast growth factors behave as mitogenic regulators for a single multipotent stem cell-like population from the subventricular region of the adult mouse forebrain. J Neurosci 1999;19:3287–3297.

23 Kukekov VG, Laywell ED, Thomas LB et al. A nestin-negative precursor cell from the adult mouse brain gives rise to neurons and glia. Glia 1997;21:399–407.

24 Keller G, Kennedy M, Papayannopoulou T et al. Hematopoietic commitment during embryonic stem cell differentiation in culture. Mol Cell Biol 1993;13:473–486.

25 Kawaguchi A, Miyata T, Sawamoto K et al. Nestin-EGFP transgenic mice: Visualization of the self-renewal and multipotency of CNS stem cells. Mol Cell Neurosci 2001;17:259–273.

26 Kaneko Y, Sakakibara S, Imai T et al. Musashi1: An evolutionally conserved marker for CNS progenitor cells including neural stem cells. Dev Neurosci 2000;22:139–153.

27 Murayama A, Matsuzaki Y, Kawaguchi A et al. Flow cytometric analysis of neural stem cells in the developing and adult mouse brain. J Neurosci Res 2002;69:837–847.

28 Shukunami C, Shigeno C, Atsumi T et al. Chondrogenic differentiation of clonal mouse embryonic cell line ATDC5 in vitro: Differentiation-dependent gene expression of parathyroid hormone (PTH)/PTH-related peptide receptor. J Cell Biol 1996;133:457–468.

29 Sakakibara S, Nakamura Y, Yoshida T et al. RNA-binding protein Musashi family: Roles for CNS stem cells and a subpopulation of ependymal cells revealed by targeted disruption and antisense ablation. Proc Natl Acad Sci U S A 2002;99:15194–15199.

30 Sakakibara S, Okano H. Expression of neural RNA-binding proteins in the postnatal CNS: Implications of their roles in neuronal and glial cell development. J Neurosci 1997;17:8300–8312.

31 Sawamoto K, Yamamoto A, Kawaguchi A et al. Direct isolation of committed neuronal progenitor cells from transgenic mice coexpressing spectrally distinct fluorescent proteins regulated by stage-specific neural promoters. J Neurosci Res 2001;65:220–227.

32 Reya T, Morrison SJ, Clarke MF et al. Stem cells, cancer, and cancer stem cells. Nature 2001;414:105–111.

33 Kobayashi M, Sjoberg G, Soderhall S et al. Pediatric rhabdomyosarcomas express the intermediate filament nestin. Pediatr Res 1998;43: 386–392.

34 Staud F, Pavek P. Breast cancer resistance protein (BCRP/ABCG2). Int J Biochem Cell Biol 2005;37:720–725.

35 Blanpain C, Lowry WE, Geoghegan A et al. Self-renewal, multipotency, and the existence of two cell populations within an epithelial stem cell niche. Cell 2004;118:635–648.

36 Morris RJ, Liu Y, Marles L et al. Capturing and profiling adult hair follicle stem cells. Nat Biotechnol 2004;22:411–417.

37 Jackson KA, Mi T, Goodell MA. Hematopoietic potential of stem cells isolated from murine skeletal muscle. Proc Natl Acad Sci U S A 1999; 96:14482–14486.

38 Torrente Y, Tremblay JP, Pisati F et al. Intraarterial injection of muscle-derived CD34(+)Sca-1(+) stem cells restores dystrophin in mdx mice. J Cell Biol 2001;152:335–348.

39 Espana EM, Kawakita T, Liu CY et al. CD-34 expression by cultured human keratocytes is downregulated during myofibroblast differentiation induced by TGF-beta1. Invest Ophthalmol Vis Sci 2004;45:2985–2991.

40 Ito CY, Li CY, Bernstein A et al. Hematopoietic stem cell and progenitor defects in Sca-1/Ly-6A-null mice. Blood 2003;101:517–523.

41 Welm BE, Tepera SB, Venezia T et al. Sca-1(pos) cells in the mouse mammary gland represent an enriched progenitor cell population. Dev Biol 2002;245:42–56.

42 Satoh M, Mioh H, Shiotsu Y et al. Mouse bone marrow stromal cell line MC3T3-G2/PA6 with hematopoietic-supporting activity expresses high levels of stem cell antigen Sca-1. Exp Hematol 1997;25:972–979.

43 Richardson GD, Robson CN, Lang SH et al. CD133, a novel marker for human prostatic epithelial stem cells. J Cell Sci 2004;117:3539–3545.

44 Corbeil D, Roper K, Hellwig A et al. The human AC133 hematopoietic stem cell antigen is also expressed in epithelial cells and targeted to plasma membrane protrusions. J Biol Chem 2000;275:5512–5520.

45 Uchida N, Buck DW, He D et al. Direct isolation of human central nervous system stem cells. Proc Natl Acad Sci U S A 2000;97:14720–14725.

46 Belicchi M, Pisati F, Lopa R et al. Human skin-derived stem cells migrate throughout forebrain and differentiate into astrocytes after injection into adult mouse brain. J Neurosci Res 2004;77:475–486.

47 Jackson KA, Majka SM, Wulf GG et al. Stem cells: A minireview. J Cell Biochem Suppl 2002;38:1–6.

48 Sosnova M, Bradl M, Forrester JV. CD34^{+} corneal stromal cells are bone marrow-derived and express hemopoietic stem cell markers. STEM CELLS 2005;23:507–515.

49 Hermann A, Gastl R, Liebau S et al. Efficient generation of neural stem cell-like cells from adult human bone marrow stromal cells. J Cell Sci 2004;117:4411–4422.

50 Anjos-Afonso F, Siapati EK, Bonnet D. In vivo contribution of murine mesenchymal stem cells into multiple cell-types under minimal damage conditions. J Cell Sci 2004;117:5655–5664.

51 Tomita Y, Matsumura K, Wakamatsu Y et al. Cardiac neural crest cells contribute to the dormant multipotent stem cell in the mammalian heart. J Cell Biol 2005;170:1135–1146.

52 Cvekl A, Tamm ER. Anterior eye development and ocular mesenchyme: New insights from mouse models and human diseases. Bioessays 2004; 26:374–386.

53 Gage PJ, Rhoades W, Prucka SK et al. Fate maps of neural crest and mesoderm in the mammalian eye. Invest Ophthalmol Vis Sci 2005;46: 4200–4208.

54 Molofsky AV, Pardal R, Iwashita T et al. Bmi-1 dependence distinguishes neural stem cell self-renewal from progenitor proliferation. Nature 2003;425:962–967.

55 Du Y, Funderburgh ML, Mann MM et al. Multipotent stem cells in human corneal stroma. STEM CELLS 2005;23:1266–1275.

56 Wroblewski J, Engstrom M, Edwall-Arvidsson C et al. Distribution of nestin in the developing mouse limb bud in vivo and in micro-mass cultures of cells isolated from limb buds. Differentiation 1997;61: 151–159.

57 Mignone JL, Kukekov V, Chiang AS et al. Neural stem and progenitor cells in nestin-GFP transgenic mice. J Comp Neurol 2004;469:311–324.

58 Zimmerman L, Parr B, Lendahl U et al. Independent regulatory elements in the nestin gene direct transgene expression to neural stem cells or muscle precursors. Neuron 1994;12:11–24.

59 Lothian C, Lendahl U. An evolutionarily conserved region in the second intron of the human nestin gene directs gene expression to CNS progenitor cells and to early neural crest cells. Eur J Neurosci 1997;9:452–462.

60 Kayahara T, Sawada M, Takaishi S et al. Candidate markers for stem and early progenitor cells, Musashi-1 and Hes1, are expressed in crypt base columnar cells of mouse small intestine. FEBS Lett 2003;535:131–135.

61 Potten CS, Booth C, Tudor GL et al. Identification of a putative intestinal stem cell and early lineage marker; musashi-1. Differentiation 2003;71: 28–41.

62 Clarke RB, Spence K, Anderson E et al. A putative human breast stem cell population is enriched for steroid receptor-positive cells. Dev Biol 2005;277:443–456.

63 Lwigale PY, Cressy PA, Bronner-Fraser M. Corneal keratocytes retain neural crest progenitor cell properties. Dev Biol 2005;288:284–293.

64 Nakamura T, Ishikawa F, Sonoda KH et al. Characterization and distribution of bone marrow-derived cells in mouse cornea. Invest Ophthalmol Vis Sci 2005;46:497–503.

65 Hamrah P, Liu Y, Zhang Q et al. The corneal stroma is endowed with a significant number of resident dendritic cells. Invest Ophthalmol Vis Sci 2003;44:581–589.

66 Beales MP, Funderburgh JL, Jester JV et al. Proteoglycan synthesis by bovine keratocytes and corneal fibroblasts: Maintenance of the keratocyte phenotype in culture. Invest Ophthalmol Vis Sci 1999;40: 1658–1663.

67 Jester JV, Barry PA, Lind GJ et al. Corneal keratocytes: In situ and in vitro organization of cytoskeletal contractile proteins. Invest Ophthalmol Vis Sci 1994;35:730–743.

68 West-Mays JA, Dwivedi DJ. The keratocyte: Corneal stromal cell with variable repair phenotypes. Int J Biochem Cell Biol 2006;38:1625–1631.

69 Rendl M, Lewis L, Fuchs E. Molecular dissection of mesenchymal-epithelial interactions in the hair follicle. PLoS Biol 2005;3:e331.

See www.StemCells.com for supplemental material available online.

nature medicine

A selective Sema3A inhibitor enhances regenerative responses and functional recovery of the injured spinal cord

Shinjiro Kaneko[1–3,9], Akio Iwanami[1,2,4,9], Masaya Nakamura[1], Akiyoshi Kishino[5], Kaoru Kikuchi[5], Shinsuke Shibata[2], Hirotaka J Okano[2], Takeshi Ikegami[1], Ayako Moriya[2], Osamu Konishi[5], Chikao Nakayama[5], Kazuo Kumagai[5], Toru Kimura[5], Yasufumi Sato[6], Yoshio Goshima[6], Masahiko Taniguchi[7], Mamoru Ito[8], Zhigang He[3], Yoshiaki Toyama[1] & Hideyuki Okano[2]

Axons in the adult mammalian central nervous system (CNS) exhibit little regeneration after injury. It has been suggested that several axonal growth inhibitors prevent CNS axonal regeneration. Recent research has demonstrated that semaphorin3A (Sema3A) is one of the major inhibitors of axonal regeneration. We identified a strong and selective inhibitor of Sema3A, SM-216289, from the fermentation broth of a fungal strain. To examine the effect of SM-216289 *in vivo*, we transected the spinal cord of adult rats and administered SM-216289 into the lesion site for 4 weeks. Rats treated with SM-216289 showed substantially enhanced regeneration and/or preservation of injured axons, robust Schwann cell–mediated myelination and axonal regeneration in the lesion site, appreciable decreases in apoptotic cell number and marked enhancement of angiogenesis, resulting in considerably better functional recovery. Thus, Sema3A is essential for the inhibition of axonal regeneration and other regenerative responses after spinal cord injury (SCI). These results support the possibility of using Sema3A inhibitors in the treatment of human SCI.

Several factors inhibit axonal regeneration after central nervous system (CNS) traumas such as spinal cord injury (SCI). Myelin-associated proteins, such as Nogo-A, myelin-associated glycoprotein (MAG) and oligodendrocyte-myelin glycoprotein (OMgp), have a central role in the inhibition of axonal regeneration[1–6]. Neutralization of Nogo receptor (NgR) signaling leads to marked axonal regeneration and functional recovery after SCI (ref. 7). In contrast, studies using Nogo knockout mice[8–10], NgR knockout mice[11,12] and other models[13–16] suggest that the blockade of axonal growth inhibitors other than myelin-associated proteins may also be important for axonal regeneration.

Among these factors, extracellular matrix molecules are likely to be important for the inhibition of axonal regrowth after SCI. CNS injury results in scar tissue formation at the injury site, which contains extracellular matrix molecules such as chondroitin sulphate proteoglycans (CSPGs)[17,18]. CSPGs are crucial as axonal growth inhibitors[17,18]: enzymatic degradation of CSPGs results in axonal regeneration and functional recovery[15]. Sema3A is another extracellular matrix molecule that may contribute to the inhibition of axonal regeneration[13,14,16] by acting on microtubules and the actin cytoskeleton[13,14,16,19–24]. In models of conditioning peripheral nerve injury, regenerating DRG axons halt selectively at Sema3A-enriched regions in the lesion site[14]. Thus, Sema3A may be a crucial extracellular factor that inhibits axonal regeneration after CNS injury. Neutralization of this molecule may hence lead to axonal regeneration and functional recovery after SCI. The high lethality of *Sema3a*$^{-/-}$ mice[22], however, has prevented close and large-scale genetic analyses of the contribution of Sema3A to the inhibitory environment of the injured spinal cord. An alternative method for large-scale analysis is to use a pharmacological approach.

Recently, we identified a small molecular agent, SM-216289, from a fungal extract, which can strongly inhibit Sema3A functions *in vitro*, including growth cone collapse and chemorepulsion of neurite extension[25,26]. SM-216289 strongly inhibits Sema3A functions *in vitro*[25,26] and SM-216289 acts directly on Sema3A to inhibit the binding of Sema3A to neuropilin-1 (NP-1), putatively by changing its steric structure. In this study, we investigated the action of SM-216289 in more detail and examined whether neutralizing Sema3A by administering SM-216289 to the injured spinal cord can create a more permissive environment for axonal regeneration *in vivo* or promote other regenerative responses, such as Schwann cell–mediated

[1]Department of Orthopaedic Surgery and [2]Department of Physiology, Keio University School of Medicine, 35 Shinanomachi, Shinjyuku-ku, Tokyo 160-8582, Japan. [3]Division of Neuroscience, Children's Hospital Boston, Harvard Medical School, 320 Longwood Avenue, Boston, Massachusetts 02115, USA. [4]Clinical Research Center, National Hospital Organization, Murayama Medical Center 2-37-1 Gakuen, Musashimurayama, Tokyo 208-0011, Japan. [5]Dainippon Sumitomo Pharma Co. Ltd., 3-1-98 Kasugade-naka, Konohana-ku, Osaka 554-0022, Japan. [6]Department of Molecular Pharmacology and Neurobiology, Yokohama City University School of Medicine, 3-9 Fukuura, Kanazawa-ku, Yokohama, Kanagawa 236-0004, Japan. [7]Department of Biochemistry, Tokyo University School of Medicine, 7-3-1 Hongo, Bunkyo-ku, Tokyo 113-0033, Japan. [8]Central Institute for Experimental Animals, 1430 Nogawa, Kawasaki, Kanagawa 216-0001, Japan. [9]These authors contributed equally to this work. Correspondence should be addressed to H.O. (hidokano@sc.itc.keio.ac.jp).

Received 24 October 2005; accepted 13 October 2006; published online 12 November 2006; doi:10.1038/nm1505

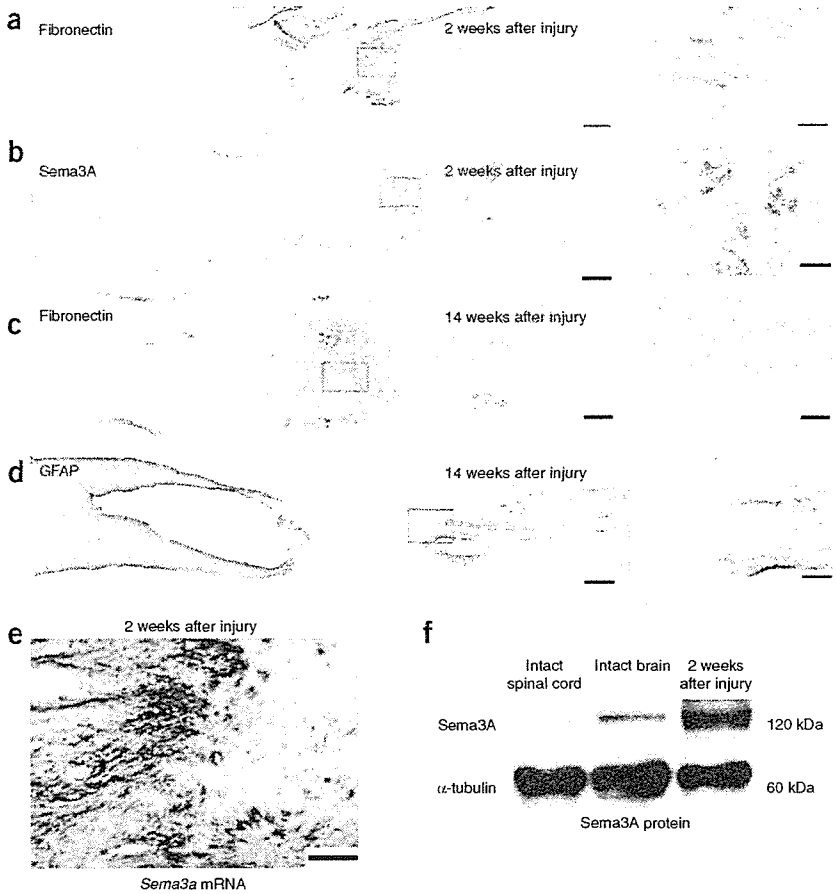

Figure 1 Expression of Sema3A after SCI. In all images, the left side is rostral. (**a–d**) Immunohistochemical analyses of the expression of fibronectin, Sema3A and GFAP in the transected spinal cord. Representative horizontal sections of the lesion site 2 weeks (**a,b**) and 14 weeks (**c,d**) after transection. Sections were stained with diaminobenzidine with nickel chloride (DAB nickel). Far right, magnified images of the boxed areas. Scale bars: 500 μm for left panels. 100 μm for right panels. (**e**) *Sema3a* mRNA expression in the lesion site 2 weeks after transection, as detected by *in situ* hybridization. Representative horizontal sections of the lesion site. Scale bar, 100 μm. (**f**) Sema3A protein expression in the lesion site as detected by immunoblotting.

myelination and axonal regeneration, inhibition of apoptosis and enhancement of angiogenesis. Our results support the potential of this Sema3A inhibitor as a therapeutic agent for human SCI patients.

RESULTS

Expression of Sema3A and other axonal growth inhibitors

In this study, we address the effect of a Sema3A inhibitor on axon regeneration in the injured spinal cord using a complete transection model. The transection model has the advantage of reproducibility, which permits a more accurate assessment of the effect of the treatment than other SCI models. Furthermore, the transection model is appropriate for the assessment of axonal regeneration. As a first step, we analyzed the spatiotemporal expression of Sema3A protein in the transected spinal cord. Two weeks after transection injury, we observed fibronectin-positive scar tissue at the lesion epicenter where Sema3A protein expression was also prominently detected (**Fig. 1a,b**). Also, 14 weeks after transection injury, the fibronectin-positive scar tissue, delineated by glial fibrillary acidic protein (GFAP)-positive glial scar tissues, extended more widely from the lesion epicenter than at 2 weeks after injury (**Fig. 1c,d**).

By *in situ* hybridization, it has been demonstrated that a marked induction of *Sema3a* mRNA takes place at the lesion site following SCI in both transection and contusion injuries[16]; *Sema3a* mRNA expression, detectable between 2 and 4 weeks after injury, was found to be colocalized with fibroblasts. Consistent with these results, we also detected high expression of *Sema3a* mRNA (by *in situ* hybridization) and Sema3A protein (by immunoblotting) (**Fig. 1e,f**). However, quantitative and temporal analyses of Sema3A protein expression after SCI have not been reported before. Therefore, we performed immunoblotting of spinal cord tissues harvested at several time points after SCI, in order to examine the temporal changes in the expression of Sema3A protein and other representative axonal growth inhibitors after spinal cord transection (**Fig. 2a–d**). We found that the expression of Sema3A protein within the transected spinal cord was upregulated at the lesion site with a peak between 1 and 2 weeks after the injury (**Fig. 2a,b**). The expression pattern of

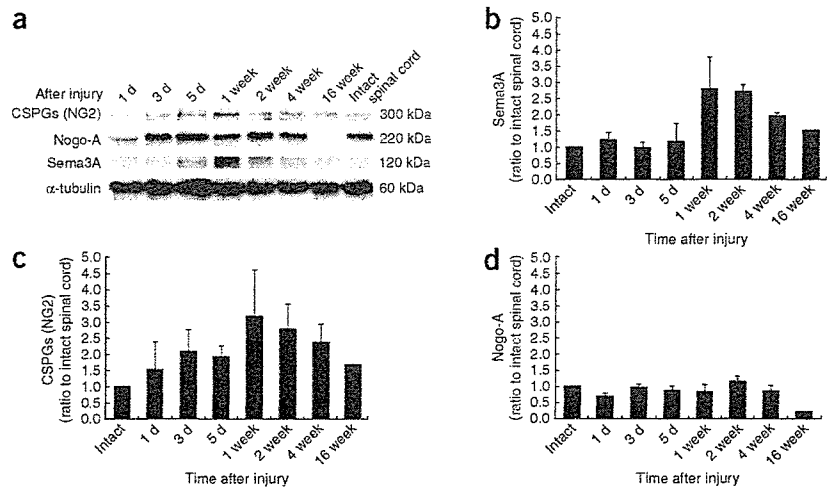

Figure 2 Temporal and quantitative analysis of Sema3A expression after SCI compared with the expression of other representative axonal growth inhibitors. (**a**) Temporal immunoblotting analysis. (**b–d**) Quantitative and temporal analysis. Data represent mean ± s.e.m.

NG2, which is representative of CSPGs upregulated after SCI, was temporally similar to that of Sema3A protein (**Fig. 2a,c**). In contrast, expression of Nogo-A, a representative myelin-associated protein, did not substantially increase within the transected spinal cord. Nogo-A expression was decreased at 16 weeks after injury, which may be partly attributable to demyelination of axons and phagocytosis of myelin debris (**Fig. 2a,d**).

Expression of NP-1 within the injured spinal cord

The receptor complex mediating Sema3A signals includes NP-1 (refs. 27–29) and plexins[30–32]. NP-1 has been reported to be the major component essential for Sema3A signaling and has a binding site for Sema3A. Therefore, we analyzed the spatiotemporal expression of NP-1 in the spinal cord after transection injury (**Supplementary Note** and **Supplementary Fig. 1** online). Considering the temporal expression patterns of Sema3A (**Fig. 2a,b**) and NP-1 (**Supplementary Fig. 1**) after injury, we administered the Sema3A inhibitor SM-216289 for 4 weeks after transection using an osmotic mini-pump (Alzet) in all subsequent experiments.

Strength and selectivity of the Sema3A inhibitor

As demonstrated previously[25,26], SM-216289 exerts a strong inhibitory effect on Sema3A. By screening various types of compounds (approximately 140,000) by growth cone collapse assay and collagen coculture assay using embroynic day (E) 7 or 8 chick DRG, we found that this compound has a maximal inhibitory effect on Sema3A. We compared SM-216289 with the tyrosine kinase inhibitor lavendustin A and the Cdk inhibitor olomoucine, which exert an inhibitory effect on Sema3A by acting intracellularly at the post-receptor level[23] (**Fig. 3a,b**). SM-216289 had a much stronger inhibitory effect on Sema3A than did either lavendustin A or olomoucine. In growth cone collapse assays, lavendustin A and olomoucine produced a minimal, if any, blockade of Sema3A-induced collapse at 1 U/ml, but not at 10 U/ml (**Fig. 3b**). In coculture assays in collagen gel, lavendustin A and olomoucine proved to have toxic effects on axonal extension at higher concentrations, unlike SM-216289 (**Fig. 3a**).

To elucidate whether SM-216289's action is selective for Sema3A, we examined (using a growth cone collapse assay) whether SM-216289 can inhibit the function of other representative axonal growth

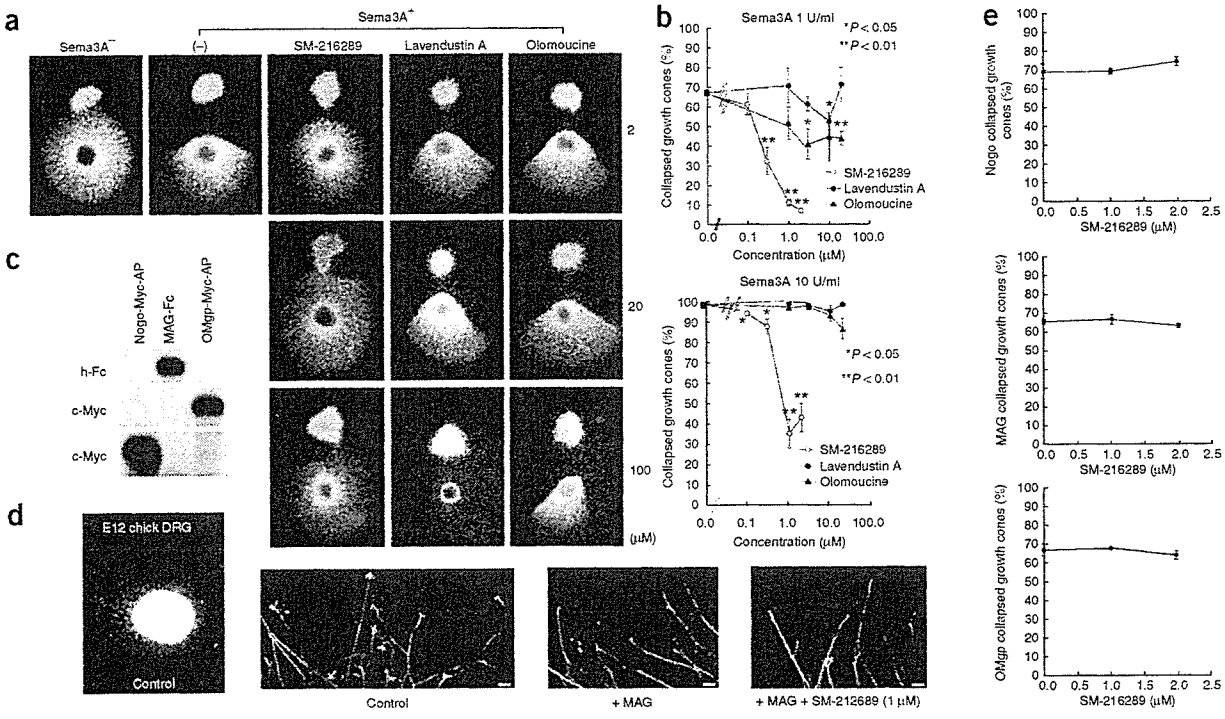

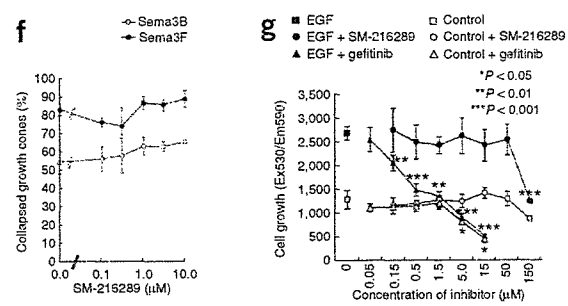

Figure 3 SM-216289 is a strong and specific Sema3A inhibitor. (**a**) Collagen coculture assay using embryonic day 8 (E8) chick DRG and Sema3A-expressing COS7 cell aggregates. SM-216289 and other compounds known to have an inhibitory effect on Sema3A, lavendustin A and olomoucine[23] were added at the indicated concentrations. (–), Sema3A with no additional compounds. (**b**) Effect of SM-216289, lavendustin A and olomoucine on growth cone collapse—induced by mouse Sema3A (1 U/ml or 10 U/ml)—in cultured E8 chick DRG. (**c**) The expression of Nogo-66-Myc-AP, MAG-Fc and OMgp-Myc-AP after transfection into HEK293T cells was confirmed by immunoblotting. (**d**) Growth cone collapse assay using E12 chick DRG. Left two panels, control growth cones. Right two panels, growth cones after incubation with MAG, with or without SM-216289. Scale bars, 20 μm. (**e**) Rate of growth cone collapse after incubation in the presence of Nogo, MAG and OMgp, and various concentrations of SM-216289. (**f**) Rate of growth cone collapse after incubation in the presence of Sema3B and Sema3F with SM-216289. (**g**) Cell growth assay using KB cells with growth dependent on epidermal growth factor (EGF). Statistical analysis: Mann-Whitney *U*-test (**a–f**) or Student's *t*-test (**g**; compared with the respective no-drug samples). Data represent mean ± s.e.m. for **b,e,f**; mean ± s.d. for **g**.

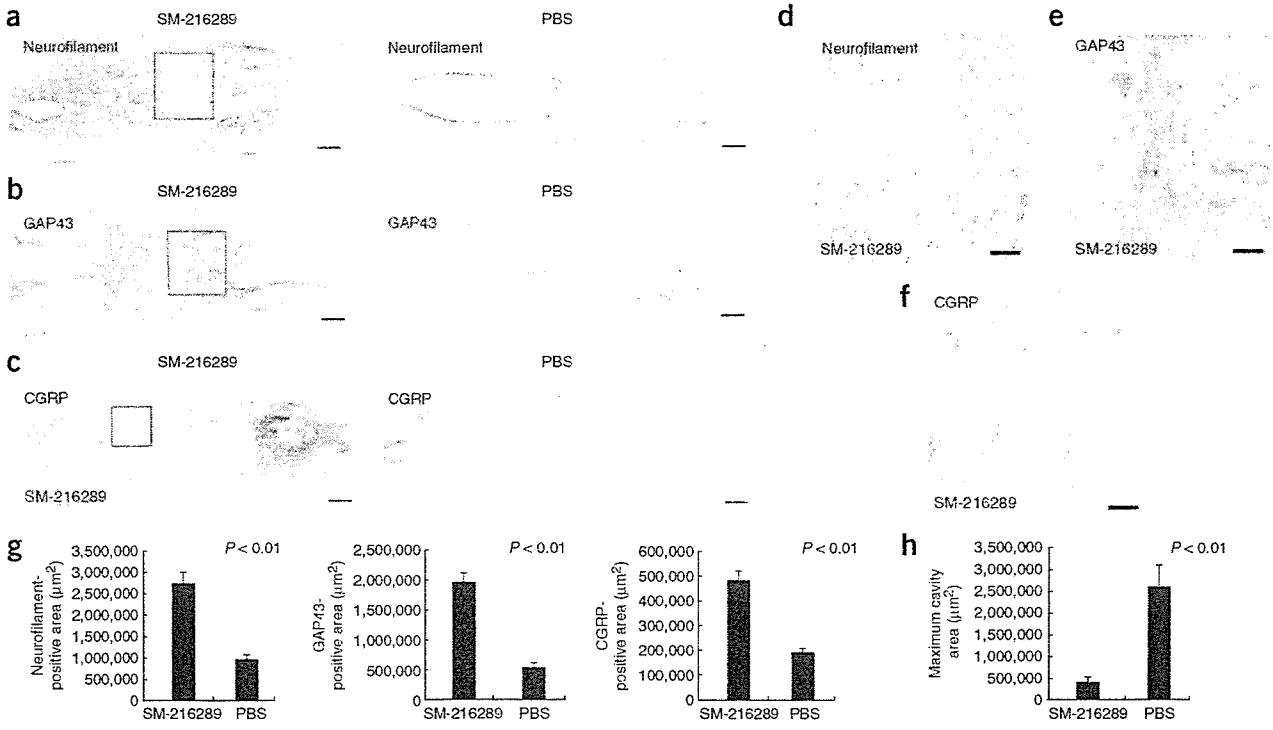

Figure 4 SM-216289 enhances axonal regeneration and reduces cavity volume in the injured spinal cord. (**a–c**) Immunohistochemical analyses of neurofilament (RT97), GAP43 and CGRP expression in the transected spinal cord. Representative horizontal sections of the lesion site 14 weeks after transection. Scale bars, 500 μm. (**d–f**) Magnified images of the boxed areas in **a–c**. The left side is rostral. Sections were stained with DAB nickel. Scale bars: 250 μm for **d**,**e**; 150 μm for **f**. (**g**) Quantitative analysis of the expression of neurofilament (RT97), GAP43 and CGRP in the transected spinal cord 14 weeks after spinal cord transection. (**h**) Quantitative analysis of the maximal dimension of the cavity area in the transected spinal cord 14 weeks after spinal cord transection. Sections were stained with DAB nickel. Statistical analysis was performed using the Mann-Whitney *U*-test. Data represent mean ± s.e.m.

inhibitors such as Nogo-A, MAG and OMgp, as well as other Sema3 family members, including Sema3B and Sema3F (ref. 20) (**Fig. 3c–f**). To prepare soluble AP-Nogo-66-Myc, MAG-Fc, AP-OMgp-Myc, Sema3A-His, AP-Sema3B and AP-Sema3F proteins, we transfected the expression plasmids into HEK293T cells and confirmed the production of these proteins in supernatants from transfected HEK293T cells by immunoblotting analysis (**Fig. 3c**). We found SM-216289 to have almost no effect on growth cone collapse induced by Nogo-66, MAG or OMgp (**Fig. 3d,e**). In addition, SM-216289 did not show any effect on the response to Sema3B and Sema3F, type-3 semaphorins related to Sema3A in sympathetic ganglia (**Fig. 3f**), demonstrating that the blockade of Sema3A by this compound is highly specific.

We examined the pharmacological profile of SM-216289 in further detail. We obtained half-maximal inhibitory concentration (IC_{50}) values for receptor and ion channel binding assays, and enzyme and kinase inhibition tests (**Supplementary Table 1** online). Overall, these IC_{50} values were much higher than the values for Sema3A (**Supplementary Table 1**). SM-216289 (30 μM) also demonstrated no agonist activity toward the receptors (data not shown).

In addition, we also used cell growth assays to determine whether SM-216289 can affect intracellular signaling pathways (**Fig. 3g**). KB cells, whose growth is dependent on epidermal growth factor (EGF), were incubated for 3 d with SM-216289 or gefitinib ('Iressa'; an EGF receptor (EGFR) inhibitor) in the absence or presence of EGF (10 ng/ml). After incubation, cell growth was measured using Alamar Blue reagent (Trek Diagnostic Systems). Both SM-216289 (0.78 μM) and gefitinib (0.02–0.08 μM) inhibited the kinase activity of EGFR in a cell-free system. Gefitinib inhibited cell growth at a range of IC_{50} values corresponding to IC_{50} values of gefitinib. In contrast, EGF-dependent cell growth was significantly affected by SM-216289 only at concentrations much higher than those required for kinase inhibition *in vitro* (**Fig. 3g**; $P < 0.01$ at 150 μM). From this cell-based assay and the profiling data (**Supplementary Table 1**), we concluded that, at expected concentrations, SM-216289 at the lesion site after drug administration has almost no cell growth– or cell function–altering effects on ion channels, receptors, intracellular signaling pathways or gene transcription in injured neurons (**Supplementary Table 1** and **Fig. 3g**). These data indicate that SM-216289 is a strong, selective agent inhibiting Sema3A and thus an excellent molecular probe for investigating the mechanism underlying Sema3A function.

We also found that SM-216289 has a strong inhibitory effect on Sema3A *in vivo* as well as *in vitro* (**Supplementary Note** and **Supplementary Fig. 2** online).

SM-216289 enhances regeneration of injured axons

To examine the effect of a degradation in Sema3A-mediated signaling on the injured axons, we administered SM-216289 into the transected spinal cords of adult rats and performed immunohistochemical analyses 14 weeks after transection using specific markers. Given that Sema3A expression in the transected spinal cord mainly lasts up to 4 weeks after injury (**Fig. 2a,c**), we administered SM-216289 or PBS for 4 weeks using an osmotic mini-pump (Alzet). By inserting the

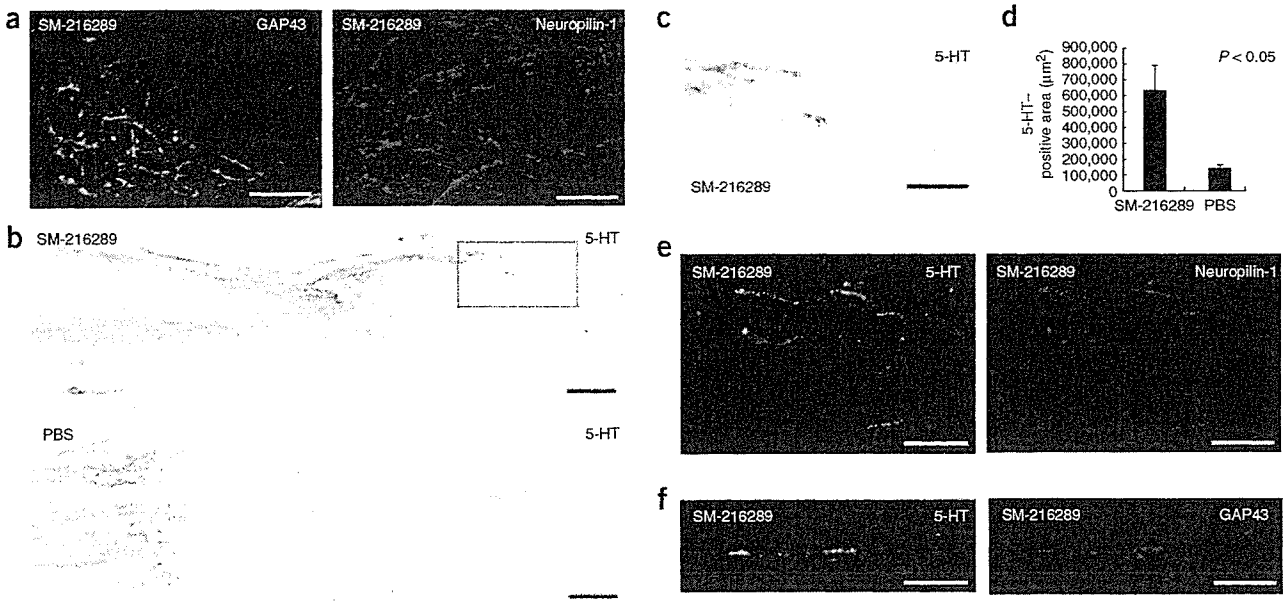

Figure 5 SM-216289 enhances axonal regeneration of NP-1–positive axons, including serotonergic (5-HT–positive) raphespinal tract axons, in the injured spinal cord. In all images, the left side is rostral. (**a**) Double-staining, in the transected spinal cord, with GAP43 and NP-1. Representative horizontal sections of the lesion site in SM-216289–administered rat. (**b**) Immunohistochemical analyses of serotonergic (5-HT–positive) raphespinal tract axons in the transected spinal cord. Representative horizontal sections of the lesion site 14 weeks after transection in SM-216289–administered and PBS-administered rats. Sections were stained with DAB nickel. (**c**) Magnified image of the boxed areas in **b**. (**d**) Quantitative analysis of expression of 5-HT in the transected spinal cord 14 weeks after spinal cord transection. (**e**) Double-staining with 5-HT and NP-1 in the transected spinal cord. Representative horizontal sections of the lesion site in SM-216289–administered rat. (**f**) Double-staining with 5-HT and GAP43 in the transected spinal cord. Representative horizontal sections of the lesion site in SM-216289–administered rat. Scale bars: 100 μm in **a**,**c**,**e**,**f**; 500 μm in **b**.

mini-pump tube just above the lesion epicenter, we ensured that SM-216289 had direct access to the lesion site. Using immunohistochemical analyses (**Fig. 4a–h**), we observed only a small number of neurofilament-positive axons within the lesion site in the control group, most probably the result of degenerative responses such as retractions. In contrast, we observed significantly more neurofilament-positive axons at the lesion site in the SM-216289–administered rats ($P < 0.01$; **Fig. 4a,d,g**). Moreover, we detected significantly more growth-associated protein 43 (GAP43)-positive axons within the lesion site in SM-216289–administered rats than in controls ($P < 0.01$; **Fig. 4b,e,g**). As GAP43 is a marker for regenerating axons, our findings suggest more robust axonal regeneration within the lesion site in the SM-216289–administered rats as compared with controls. Furthermore, most of the GAP43-positive axons expressed NP-1, suggesting that these axons can respond to both Sema3A and SM-216289 (**Fig. 5a**). However, it is also possible that the observed phenotypes resulting from the administration of SM-216289 are due to the enhanced preservation of injured axons. We next decided to characterize the axons in the lesion site more extensively. The sprouting of peptidergic nociceptive C fibers within the spinal cord after injury enhances several debilitating responses, such as neuropathic pain and autonomic dysreflexia[33]. We used a representative marker for these C-fiber axons, calcitonin gene–related peptide (CGRP), and observed significantly more CGRP-positive axons at the lesion site of SM-216289–administered rats as compared to controls ($P < 0.01$). However, the number of CGRP-positive neurons was very limited overall when compared with neurofilament-positive or GAP43-positive axons in the lesion site (less than one-fourth; **Fig. 4c,f,g**). Furthermore, previous reports have indicated that the abnormal sensory functions primarily result from the sprouting of uninjured CGRP-positive axons rather than injured CGRP-positive axons[34,35]. Considering the nature of the transection model in our experiment, most of the CGRP-positive axons we observed were most probably injured axons that had regenerated. However, there may have been some CGRP-positive axons adjacent to the lesion site that had not been transected, because CGRP-positive axons could originate from dorsal roots that enter the spinal cord rostral to the lesion site. To avoid including such uninjured axons, we counted axons only within the lesion site. In addition, paw withdrawal tests[34,35] did not show any allodynia (data not shown), suggesting that SM-216289 treatment is not likely to induce abnormal sensory function in this model. Parvalbumin (PV)-positive neurons are known to be proprioceptive sensory neurons, and it is possible that these neurons may have additional beneficial effects on behavioral function. By double-immunostaining for GAP43 and PV, we observed PV-positive axons among the regenerated axons (**Supplementary Fig. 3** online). However, the overall number of both CGRP-positive and PV-positive axons was limited, indicating that sensory neurons are not likely to be the major population among the regenerated axons. We did not observe the regeneration of ascending dorsal column axons (**Supplementary Fig. 3**) or the descending corticospinal tract (CST) through the lesion site in SM-216289–administered rats, consistent with the results from *Sema3a*$^{-/-}$ mice (data not shown). Notably, although we did not observe robust regeneration of serotonergic (that is, 5-hydoxytryptamine (5-HT)-positive) descending raphespinal tract axons[11,36] in the spinal cord in locations far caudal to the lesion site, 5-HT–positive axons appeared to cross the lesion site quite abundantly (inside the scar tissue) in the SM-216289–administered group (**Fig. 5b–d**). We

also confirmed that these serotonergic (5-HT–positive) raphespinal tract axons at the lesion site in the SM-216289–administered group expressed NP-1 (**Fig. 5e**) and GAP43 (**Fig. 5f**).

SM-216289 enhances Schwann cell migration

We also performed electron microscopic and immunohistochemical analyses to examine whether the regenerated axons become myelinated (**Fig. 6a,b**). We observed that most of the regenerated axons were myelinated in rats administered SM-216289, which was rarely seen in control rats (**Fig. 6b**). Notably, the myelination of the regenerated axons seemed to be of the peripheral type, which is characterized by the presence of Schwann cells, perineuria and basal lamina. This peripheral-type myelination indicates that Schwann cells migrate into the lesion site[37–39], and that these cells contributed to the myelination of regenerating fibers more extensively in the SM-216289–administered rats than in control rats. Therefore, we performed immunohistochemistry against P0, a representative marker of Schwann cells[40], and confirmed that migrated Schwann cells exist

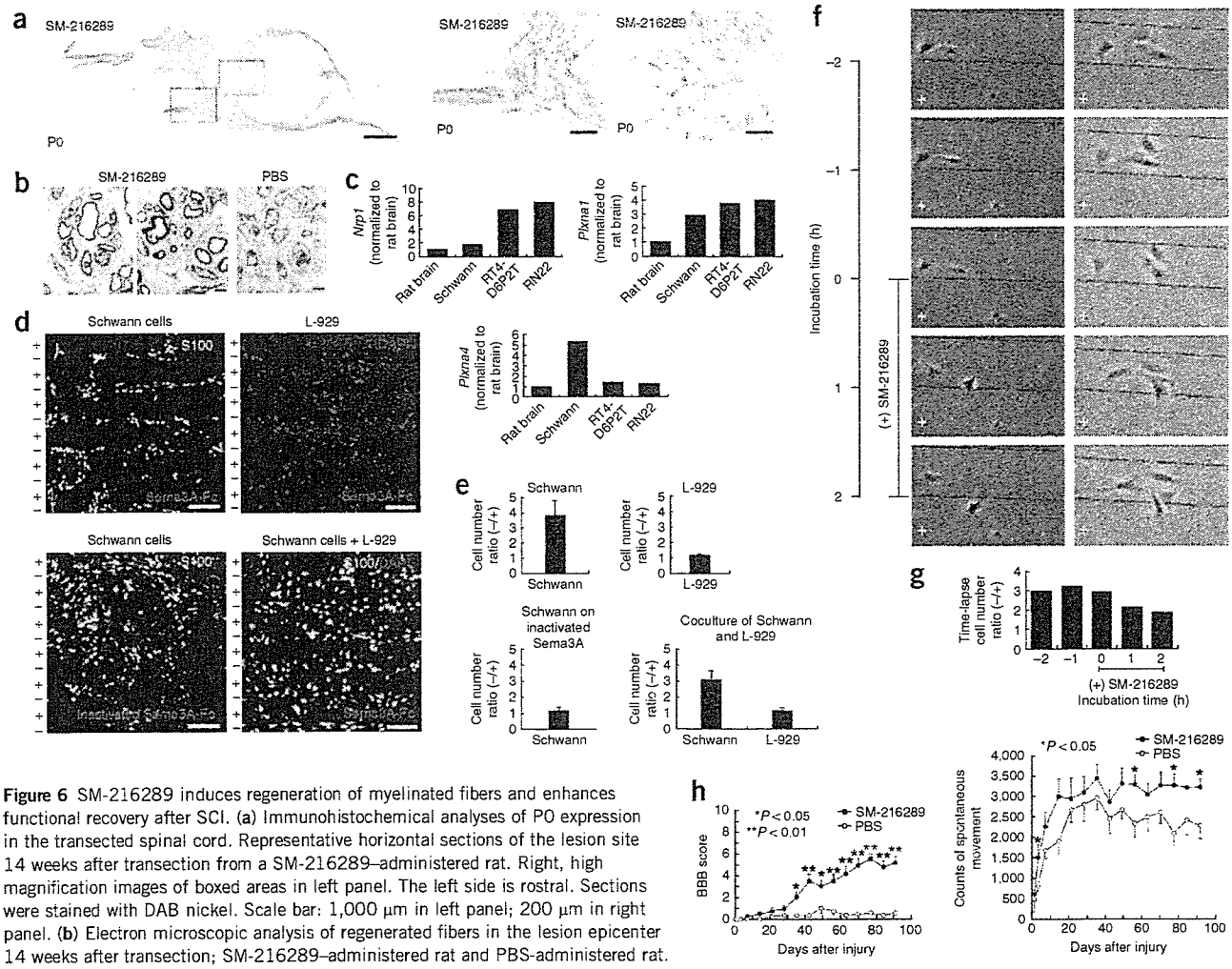

Figure 6 SM-216289 induces regeneration of myelinated fibers and enhances functional recovery after SCI. (**a**) Immunohistochemical analyses of P0 expression in the transected spinal cord. Representative horizontal sections of the lesion site 14 weeks after transection from a SM-216289–administered rat. Right, high magnification images of boxed areas in left panel. The left side is rostral. Sections were stained with DAB nickel. Scale bar: 1,000 μm in left panel; 200 μm in right panel. (**b**) Electron microscopic analysis of regenerated fibers in the lesion epicenter 14 weeks after transection; SM-216289–administered rat and PBS-administered rat. Representative transverse sections of the lesion epicenter. Scale bars, 2 μm. (**c**) Expression of Sema3A receptor components in Schwann cells. Total RNA was prepared from rat brain, primary Schwann cells and two Schwann cell–derived cell lines, and mRNA expression of *Nrp1*, *Plxna1* and *Plxna4* were analyzed with quantitative RT-PCR. Data normalized to expression level of rat brain are shown. (**d**) Schwann cells migration stripe assay. Schwann cells avoided stripes of immobilized Sema3A. Top left, Schwann cells were cultured on stripes of Sema3A-Fc and visualized in green by antibody to S100 (anti-S100; green). Top right, cells of the fibroblast cell line L-929, which do not express NP-1, were cultured on stripes of Sema3A-Fc and visualized by nuclei staining with 4′,6-diamidino-2-phenylindole (DAPI; blue). Bottom left, Sema3A-Fc was heat inactivated (65 °C, 30 min) before coating. Bottom right, a mixture of Schwann and L-929 cells was cultured on stripes of Sema3A-Fc and double-stained with anti-S100 (green) and DAPI (blue). Schwann cells were stained with anti-S100 (green, with blue nuclei); in contrast, L-929 cells were visualized only by their blue nuclei. Scale bars, 200 μm. (**e**) Ratio of the cell density between areas coated and noncoated with Sema3A-Fc. Bottom right, ratio of the cell density determined for Schwann cells and L-929 cells independently. Data represent mean ± s.d. (**f**) SM-216289 attenuates the Sema3A avoidance exhibited by Schwann cells. After preincubation (16 h), Schwann cells were incubated for 2 h before ($T = -2$ h to 0 h) and after ($T = 0$ h to 2 h) addition of SM-216289 (to be 200 μM as final concentration). Time-lapse photographs taken every hour (–2 h to 2 h) (two representative cell samples—one sample in each column—at each time point; arrowheads within a column indicate one particular cell within the sample). $T = 0$, time point at which SM-216289 was added to the culture. +, Sema3A-coated areas. Lines, boundaries of Sema3A-coated areas. (**g**) Relative cell densities (cell number ratio) at indicated time points in the time-lapse analysis. (**h**) Temporal functional analysis using BBB scoring (left) and temporal analysis of spontaneous movement using SCANET (right) up to 14 weeks after transection. Statistical analysis was performed using the Mann-Whitney *U*-test. Data are mean ± s.e.m.

abundantly in the lesion site in the SM-216289–administered group (**Fig. 6a**). We also confirmed the robust expression of *Nrp1*, *Plxna1* and *Plxna4* mRNA in Schwann cells using quantitative RT-PCR (**Fig. 6c**), suggesting that Schwann cells have the ability to respond to Sema3A or SM-216289. Also, using Sema3A-Fc fusion stripe assays, we found that Sema3A had a substantial repulsive effect on Schwann cell migration (**Fig. 6d,e**). When Schwann cells were cultured on the Sema3A stripe (made on a poly-L-ornithine substrate), Schwann cells avoided Sema3A-coated areas and preferentially distributed upon Sema3A-noncoated areas (**Fig. 6d,e**). The ratio of cell density between Sema3A-noncoated and Sema3A-coated areas ($Sema3A^-/Sema3A^+$) was 3.78 ± 0.98 (mean ± s.d.) in this experimental condition. To assess whether the behavior of Schwann cells depends on Sema3A signaling, we also examined the behavior of a Sema3A-insensitive fibroblast cell line, L-929, which does not express *Nrp1* mRNA (**Supplementary Fig. 4** online), on the same stripe as a negative control (in a pilot experiment, we confirmed using quantitative RT-PCR that the L-929 cells do not express *Nrp1* mRNA, although they do express *Plxna1* and *Plxna4* mRNA (**Supplementary Fig. 4**); therefore, they cannot respond to Sema3A). L-929 cells were randomly distributed on both Sema3A-coated and Sema3A-noncoated areas ($Sema3A^-/Sema3A^+$ = 1.17 ± 0.15). We also did not observe the avoiding behavior of Schwann cells on heat-inactivated Sema3A-Fc ($Sema3A^-/Sema3A^+$ = 1.18 ± 0.19; **Fig. 6d,e**). To confirm cell type–specific behavior on Sema3A stripes more directly, we cultured both Schwann cells and L-929 cells on these stripes. Schwann cells, but not L-929 cells, did not remain on Sema3A ($Sema3A^-/Sema3A^+$ = 3.05 ± 0.53 in Schwann, 1.19 ± 0.08 in L-929; **Fig. 6d,e**). These results clearly show that Schwann cells are sensitive to Sema3A and are repelled by Sema3A-coated areas. To examine more dynamically whether SM-216289 attenuates the repulsive effect of Sema3A against Schwann cells, we performed a time-lapse video analysis. Schwann cells were cultured on a Sema3A stripe for 16 h, and, using time-lapse video microscopy, we recorded the cell distribution on the stripe for 2 h before and after SM 216289 treatment. The population of cells that remained on Sema3A-noncoated areas markedly decreased even 1 h after SM-216289 treatment (**Fig. 6f,g**). This result suggests that inhibition of Sema3A can rapidly trigger Schwann cell migration into Sema3A-coated areas.

Presumably, the presence of peripheral-type myelin, which does not contain axonal growth inhibitors such as Nogo-A and OMgp (refs. 1–3,5,6), may contribute to the enhanced axonal regeneration observed. Our findings indicate that SM-216289 administration downregulates Sema3A signaling, upregulates regeneration-associated proteins in injured neurons and promotes Schwann cell–mediated myelination and axonal regeneration in the lesion site (**Figs. 4,5,6a–g**).

SM-216289 inhibits apoptosis and enhances angiogenesis

We found that SM-216289 also has a neuroprotective effect on cells at the lesion site after spinal cord transection injury (**Supplementary Note** and **Supplementary Fig. 5** online).

We also found enhanced angiogenesis at the lesion site in the SM-216289–administered rats (**Supplementary Note** and **Supplementary Fig. 5**).

SM-216289 promotes functional recovery after SCI

To examine the effect of SM-216289 on the rats' behavioral functions, we used the 21-point open-field Basso-Beattie-Bresnahan (BBB) locomotor rating scale (BBB scoring) to assess hindlimb movement[41] and the automated animal movement analysis system (SCANET) to measure spontaneous movement[42] of the rats. Hindlimb movement was significantly enhanced by the administration of SM-216289 (**Fig. 6h**; $P < 0.05$ at 5 and 7 weeks after injury; $P < 0.01$ at 6, 8, 9, 10, 11, 12 and 13 weeks after injury). In all the rats used in this study, hindlimb movement was abolished immediately after transection. Whereas hindlimb paralysis showed virtually no recovery in control rats (average BBB score: 0.55 ± 0.21 (mean ± s.e.m.) at 14 weeks after injury), hindlimb movement improved significantly in SM-216289–administered rats from 5 to 14 weeks after transection injury (average BBB score: 5.13 ± 0.57 at 14 weeks after injury). We also confirmed that the functional recovery resulted from the regeneration of axons in the lesion site rather than from recovery of autonomous function in the spinal cord below the lesion. For this purpose, the lesion site was retransected 10 weeks after the first transection, which resulted in a loss of recovered behavioral function (**Supplementary Fig. 6** online). The retransected rats' BBB scores dropped to 0 and remained at or below 1 for at least 5 weeks ($n = 5$). These retransection experiments suggested that the significant functional recovery observed in the treatment group was most probably caused by regeneration across the lesion site and not by compensatory response below the lesion site. Furthermore, we also found that by disrupting the serotonergic (5-HT–positive) raphespinal tract using the serotonin neurotoxin 5,7-dihydroxytryptamine (DHT) as previously described[11], the functional recovery observed in the SM-216289–administered group ($P < 0.05$ at 4, 9 and 10 weeks after injury; $P < 0.01$ at 6, 7 and 8 weeks after injury) could be substantially attenuated (**Supplementary Fig. 6**). This suggested that the enhanced regeneration of serotonergic (5-HT–positive) raphespinal tract was at least partly responsible for the improved functional recovery observed in the SM-216289–administered group.

Spontaneous movement was also significantly enhanced in the SM-216289–administered rats when compared with control rats ($P < 0.05$ at 3 d and 8, 11 and 13 weeks after injury; **Fig. 6h**). However, at some early time point, we observed a significant difference in spontaneous movement that was not reflected in BBB scores (**Fig. 6h**), indicating that the observed early effects of SM-216289 may have resulted from mechanisms other than axonal regeneration across the lesion site—for instance, local neuroprotective effects.

DISCUSSION

The current study has two major findings: first, that Sema3A contributes considerably to the inadequate axonal regeneration at the spinal cord lesion site after transection injury; and second, that SM-216289 strongly inhibits the Sema3A signal both *in vivo* and *in vitro*, and is an effective promoter of regenerative responses including axonal regeneration and/or preservation, Schwann cell–mediated myelination and axonal regeneration, angiogenesis, and the inhibition of apoptosis after spinal cord transection.

The involvement of Sema3A in an *in vivo* experimental animal model of SCI has been described in several reports[13,14,16]. For instance, a previous study showed using *in situ* hybridization that *Sema3a* mRNA expression is upregulated within the fibronectin-positive scar tissue following transection and contusion injuries in the adult rat spinal cord. The same study also showed that two major descending spinal cord motor pathways, the corticospinal and rubrospinal tracts, continue to express mRNA of receptor components for Sema3A after injury, suggesting that these axon tracts may be potentially sensitive to Sema3A within the scar tissue. Consistently, most descending fibers did not penetrate the *Sema3a* mRNA–expressing portion of the scar tissue at the lesion site[16]. These results suggest that Sema3A contributes to the inhibitory properties of the scar tissue, thereby inhibiting successful regeneration of injured axons.

These findings, however, do not provide direct evidence that Sema3A contributes significantly to the inhibitory properties of the lesion site in the spinal cord after injury. But as mentioned earlier, because the high lethality of *Sema3a*$^{-/-}$ mice precludes an adequate genetic assessment of the contribution of Sema3A to the limited regeneration of the injured spinal cord, we decided to use a pharmacological approach as an alternative method. In this study, neutralizing Sema3A created a permissive environment for the regeneration of injured spinal cord axons. Our findings thus indicate more directly that Sema3A contributes substantially to the inhibitory properties of the lesion site in the spinal cord after transection. However, we also observed that in SM-216289–administered rats, there was no axonal regeneration of long axon tracts other than 5-HT–positive raphespinal tract axons (which include CST and ascending dorsal column fibers), consistent with the results from *Sema3a*$^{-/-}$ mice. Our data thus indicate that the contribution of Sema3A to regenerative incompetency is considerable but limited.

There are several possible explanations for the markedly enhanced functional recovery observed in SM-216289–administered rats. Although we detected the enhanced regeneration and/or preservation of axons in the lesion site, we did not observe that axons in some long axon tracts such as the CST penetrated the lesion site (**Figs. 4** and **5**). However, past studies using complete transection injury models have rarely provided convincing evidence of corticospinal tract regeneration, most probably due to the existence of a gap of a few millimeters between the severed ends of the spinal cord (which results in enormous scar tissue area) in the lesion site after transection injury. Notably, although we did not observe extensive serotonergic raphespinal tract axons[11,36] in the spinal cord at locations far caudal to the lesion site in either group, we did identify considerably more 5-HT–positive axons within and across the lesion site (**Fig. 5b–d**) in the SM-216289–administered group. Furthermore, we also found that by disrupting the serotonergic raphespinal tract using 5,7-DHT as previously described[11], the functional recovery observed in the SM-216289–administered group could be markedly attenuated, which suggests that a considerably enhanced regeneration of raphespinal tract fibers may be at least partly responsible for the improved functional recovery observed in this group. It has been reported that disrupting Nogo receptor signaling using genetic approaches could promote the regeneration of serotonergic raphespinal tract axons across the lesion site into the side far caudal to the lesion site[11]. Therefore, it is possible that in order to obtain further regeneration of serotonergic fibers in the raphespinal tract, inhibitory signals other than Sema3A may also need to be disrupted.

It is also plausible that the regenerated axons observed in the lesion site of SM-216289–administered rats may include preserved and regenerated short projection neurons or interneurons. The increased number of axons in the lesion site in the SM-216289–administered group may have arisen from enhanced neuroprotection, which protects axons from retraction or degeneration and gives them a higher probability of regeneration. A recent study reported that regenerating local axons, consisting mainly of interneurons, can form intraspinal neural circuits in the lesion site after spinal cord injury and make synaptic connections with CST collaterals[43]. Although this study used a hemisection model, which is different from our current model, it is plausible that this kind of mechanism, with signal relay via short regenerated neuronal fibers, may also be responsible for the functional recovery[43]. In addition, our retransection experiments suggest that the functional recovery observed in the treatment group is most probably caused by regeneration within and across the lesion site, and not by compensatory responses below the lesion site.

A second possible mechanism involves the enhancement of Schwann cell migration by SM-216289 administration, along with a guidance role for Schwann cells in axonal regeneration and in the promotion of myelination of the regenerated fibers. Sema3A has been reported to be involved in some forms of cell migration[37–39]. In SM-216289–administered rats, most of the regenerated axons were myelinated by Schwann cells, an observation rarely made in control rats (**Fig. 6b**). These findings indicate that Schwann cells had extensively migrated into the lesion site in SM-216289–administered rats, that they had guidance roles in axonal regeneration and that they contributed to the myelination of regenerated fibers. In support of this hypothesis, we confirmed the robust expression of *Nrp1*, *Plxna1* and *Plxna4* mRNA in Schwann cells (by quantitative RT-PCR) (**Fig. 6c**). Using an *in vitro* stripe assay, we also found that Sema3A repels Schwann cells (**Fig. 6d,e**) and, furthermore, that SM-216289 attenuates this repulsive response (**Fig. 6f,g**). These results support the hypothesis that Schwann cell migration into the lesion site may be affected by Sema3A activity. Also, considering a previous report describing the effect of Sema3A on neural crest cell migration[37], it is also possible that immature neural crest–derived cells putatively present in the peripheral nerve[44] can migrate into the lesion site within the injured spinal cord, where they may then mature into Schwann cells. This peripheral-type myelination, which does not involve axonal growth inhibitors such as Nogo-A and OMgp, is considered to be favorable for axonal regeneration and may play a guidance role in axonal regeneration.

Two other potential mechanisms are discussed in the **Supplementary Discussion** online. We consider these and the two possibilities discussed above to be the major mechanisms that may be responsible for the functional recovery observed in this study.

As mentioned earlier, studies using Nogo[8–10] and Nogo receptor knockout mice[11,12], as well as other reports[13–16], support the idea that axonal growth inhibitors other than myelin-associated proteins are present, and that these must be overcome for adequate axonal regeneration to occur. Among them, extracellular matrix molecules have been regarded as key molecules limiting axonal regeneration after SCI.

In this study, we targeted Sema3A (refs. 13,14,16,19–24), which, in addition to CSPGs (refs. 15,17,18), has been reported to be a major extracellular matrix molecule inhibiting axonal regeneration. We consequently demonstrated that SM-216289 (refs. 25,26) can strongly and selectively inhibit Sema3A signaling both *in vitro* and *in vivo*, and, most importantly, provided evidence that this compound is a potentially effective agent for promoting axonal regeneration after spinal cord transection.

To achieve further axonal regrowth, including the regeneration of long fiber tracts, the concomitant use of SM-216289 with other therapeutic modalities such as neurotrophic factors[45], soluble Nogo receptors[7], chondroitinase ABC (ref. 15), or tissue or cell transplantation[36], could potentially be beneficial. As a model for SCI, the transection protocol is appropriate for assessing axonal regeneration, but it does not fully parallel SCI in the clinical setting. In contrast, the contusion model may be more representative of human SCI because it reveals features similar to those seen in the clinical context. Therefore, future studies should focus on the concurrent use of SM-216289 with other treatments, its application to contusion lesions, or its application to nonhuman primates. In conclusion, this study demonstrates that Sema3A plays an essential role in regenerative failure (including the inhibition of axonal regeneration) after SCI and that SM-216289 may be a possible therapeutic agent for human SCI.

METHODS

Animals and surgical procedures. We used adult female Sprague-Dawley rats weighing 200–250 g in this study. All aspects of animal care and treatment were carried out according to the guidelines of the experimental animal care committee of Keio University, School of Medicine. Anesthetized (sodium pentobarbital, 40 mg per kg body weight) rats received complete spinal cord transections at the Th8 lamina level using procedures described previously[36]. Briefly, after Th8 laminectomy, the dura was opened, and the spinal cord was transected using a surgical blade (Feather). The severed ends of the cord typically retracted about 3 mm and were inspected under a surgical microscope to ensure complete transection. The muscles and skin were closed in layers. The administration of SM-216289 is described in detail in a later section. After the operation, the rats were kept warm, placed on beds of sawdust, and given manual bladder evacuation twice per day and intramuscular injection of ampicillin (50 mg once per day up to 1 week after transection) to prevent infections. To prevent dehydration, rats were hydrated with up to 20 ml per day of lactated Ringer's solution or normal saline injected intraperitoneally (i.p.). Food was provided on the cage floor, and the rats had no difficulty reaching their water bottles. Supplemental oral feedings were given as necessary. Surgeries for retransection were performed 10 weeks after the first transection in the same manner ($n = 5$).

For axon tract tracing, rats received six stereotaxic injections of 10% biotinylated dextran amine (BDA, Molecular Probes) in the sensorimotor cortex of the bilateral forelimb and hindlimb region ($n = 6$) 8 weeks after the transection injury. For each injection, 0.5 μl BDA was delivered over a period of 2 min by means of a glass pipette (inner diameter 10–15 μm) attached to a nanoinjector (Stoelting). These BDA-injected rats were killed 14 d after the injection. Nine weeks after transection, cholera toxin B subunit (CTB, 1%, List Biological Lab) was injected into the sciatic nerves bilaterally ($n = 4$). For each injection, 5 μl CTB was delivered over a period of 20 s by means of a glass pipette (inner diameter 10–15 μm) attached to the nanoinjector (Stoelting). These CTB-injected rats were killed 5 d after the injection.

For the rats receiving bilateral intracerebroventricular (i.c.v.) injections of the serotonin neurotoxin DHT (300 μg dissolved in 5 μl of 0.2% ascorbic acid in normal saline), the procedure was performed as described[11] with slight modification 10 weeks after complete transection ($n = 8$: 4 each in the SM-216289 and PBS groups). Thirty minutes before the 5,7-DHT injection, we administered the monoamine uptake inhibitor desipramine (25 mg/kg, i.p.; Sigma).

In this study, we also used *Sema3a*-deficient mice as described in a previous report[22]. We obtained *Sema3a*$^{-/-}$ homozygous mutant mice through *in vitro* fertilization and applied almost identical surgical procedures as described above for rats to the *Sema3a*$^{-/-}$ mice and control wild-type C57/BL6 mice, using smaller dosages of tracers.

See **Supplementary Methods** online for details of the primary antibodies used; the immunohistochemistry, *in situ* hybridization and immunoblotting procedures; the preparation of SM-216289 by fermentation of the *Penicillium* sp. strain SPF-3059; the pharmacological profiling of SM-216289; and the cell growth assay.

Quantification for immunohistochemistry. Quantification of each marker's immunoreactive density was performed using the MCID Elite System (Imaging Research Inc.) as described[46] with slight modifications[47,48]. Details are available in the **Supplementary Methods**.

Growth cone collapse assay. The growth cone collapse assay was performed as described in ref. 20 with slight modifications[23,25]. Details are available in the **Supplementary Methods**.

Co-culture assay in collagen gel. Collagen co-culture experiments were performed as described previously[49] with slight modifications[25]. Details are available in **Supplementary Methods**.

Administration of SM-216289 into the injured spinal cord. At the time of transection injury, we placed an osmotic mini-pump (Alzet) underneath the back skin and guided the attached tube into the lesion site. We performed this tubing procedure so that the exit from the osmotic mini-pump's tube was set just above the lesion epicenter, thus ensuring that SM-216289 had direct access to the lesion. We administered SM-216289 (0.1 mg/ml, 0.174 mM) through the osmotic mini-pump for 4 weeks (0.25 μl/h, 0.6 μg/d) after the injury. For the control rats, we delivered the same amount of PBS instead of SM-216289.

After the administration of SM-216289 into the injured spinal cord, we conducted an immunoblotting analysis of the molecules downstream of Sema3A, and also analyzed the apoptotic cells. Details of both procedures are in **Supplementary Methods**, along with information pertaining to the electron microscopic analysis, quantitative RT-PCR and behavioral analysis.

Schwann cell migration stripe assay. Schwann cells were prepared from sciatic nerves of P7 Wistar rats as described[50] with slight modifications. Details are available in the **Supplementary Methods**.

Note: Supplementary information is available on the Nature Medicine website.

ACKNOWLEDGMENTS

We are grateful to L. Benowitz (Children's Hospital Boston); H. Fujisawa (Nagoya University); A.L. Kolodkin (Johns Hopkins University); and Y. Ihara and K. Mori (Tokyo University) for reagents. We also thank M. Dezawa, S. Kawabata, U. Uchida, Y. Sugiyama, F. Nakamura, T. Nagai, S. Miyao, T. Harada, K. Watanabe, H. Hanafusa, Y. Ujimasa, T. Yagi and G. Yiu for technical assistance. We are also grateful to T. Takahashi, H. Fujisawa and F. Murakami for their critical reading of the manuscript, to the members of the Okano Laboratory for their comments on the manuscript. This work was supported by grants from the Leading Project for Realization of Regenerative Medicine from the Ministry of Education, Culture, Sports, Science and Technology (MEXT), Japan; the Japan Science and Technology Corporation (JST); and the General Insurance Association of Japan. This work was also supported by a Keio University special grant-in-aid for innovative collaborative research projects to H.O.; a Keio University grant-in-aid for encouragement of young medical scientists to S.K. and A.I.; and a grant-in-aid from the 21st Century COE Program of MEXT, Japan, to Keio University.

AUTHOR CONTRIBUTIONS

S.K. wrote the manuscript, conducted all the SCI experiments (including preparation of the SCI model rats, and behavioral and histochemical characterizations), conducted *in vitro* assays (including growth cone collapse assay) and all the immunoblotting, and prepared the recombinant proteins. A.I. conducted rat SCI experiments as detailed above, conducted SCI experiments of *Sema3a*-deficient mice, and cowrote the manuscript. M.N. instructed S.K. and A.I. on the technical aspects of the SCI experiments, and cowrote the manuscript. A.K. conducted histochemical characterization of SCI model rats. K. Kikuchi conducted *in vitro* experiments (including collagen gel coculture, KB-cell cell growth assay and Schwann cell migration assay). S.S. conducted cell preparation for the *in vitro* migration assay. H.J.O. prepared the recombinant proteins. T.I. participated in SCI experiments including behavioral characterizations. A.M. prepared the recombinant semaphorin proteins. O.K participated in histochemical characterization of SCI model rats. C.N. organized the collaboration with Keio University at Dainippon Sumitomo. K. Kumagai prepared SM-216289 and examined its specificity of action *in vitro*. T.K. supervised the SM-216289 project at Dainippon Sumitomo. Y.S. and Y.G. examined the specificity of SM-216289's effect on Sema3A by growth cone collapse assay. M.T. provided and conducted the genetic diagnosis of *Sema3a*-deficient mice. M.I. conducted the *in vitro* fertilization of *Sema3a*-deficient mice. Z.H. provided advice on the experimental design. Y.T. supported and supervised the SCI experiments conducted at Keio University. H.O. supervised the whole project and cowrote the manuscript with S.K., A.I. and M.N.

COMPETING INTERESTS STATEMENT

The authors declare that they have no competing financial interests.

Published online at http://www.nature.com/naturemedicine
Reprints and permissions information is available online at http://npg.nature.com/reprintsandpermissions/

1. Schwab, M.E., Kapfhammer, J.P. & Bandtlow, C.E. Inhibitors of neurite growth. *Annu. Rev. Neurosci.* **16**, 565–595 (1993).
2. GrandPre, T., Nakamura, F., Vartanian, T. & Strittmatter, S.M. Identification of the Nogo inhibitor of axon regeneration as a reticulon protein. *Nature* **403**, 439–444 (2000).
3. Chen, M.S. *et al.* Nogo-A is a myelin-associated neurite outgrowth inhibitor and an antigen for monoclonal antibody IN-1. *Nature* **403**, 434–439 (2000).

4. Domeniconi, M. *et al.* Myelin-associated glycoprotein interacts with the Nogo66 receptor to inhibit neurite outgrowth. *Neuron* **35**, 283–290 (2002).
5. Olson, L. Medicine: clearing a path for nerve growth. *Nature* **416**, 589–590 (2002).
6. Wang, K.C. *et al.* Oligodendrocyte-myelin glycoprotein is a Nogo receptor ligand that inhibits neurite outgrowth. *Nature* **417**, 941–944 (2002).
7. Li, S. *et al.* Blockade of Nogo-66, myelin-associated glycoprotein, and oligodendrocyte myelin glycoprotein by soluble Nogo-66 receptor promotes axonal sprouting and recovery after spinal injury. *J. Neurosci.* **24**, 10511–10520 (2004).
8. Kim, J.E., Li, S., GrandPre, T., Qiu, D. & Strittmatter, S.M. Axon regeneration in young adult mice lacking Nogo-A/B. *Neuron* **38**, 187–199 (2003).
9. Simonen, M. *et al.* Systemic deletion of the myelin-associated outgrowth inhibitor Nogo-A improves regenerative and plastic responses after spinal cord injury. *Neuron* **38**, 201–211 (2003).
10. Zheng, B. *et al.* Lack of enhanced spinal regeneration in Nogo-deficient mice. *Neuron* **38**, 213–224 (2003).
11. Kim, J.E., Liu, B.P., Park, J.H. & Strittmatter, S.M. Nogo-66 receptor prevents raphespinal and rubrospinal axon regeneration and limits functional recovery from spinal cord injury. *Neuron* **44**, 439–451 (2004).
12. Zheng, B. *et al.* Genetic deletion of the Nogo receptor does not reduce neurite inhibition *in vitro* or promote corticospinal tract regeneration *in vivo*. *Proc. Natl. Acad. Sci. USA* **102**, 1205–1210 (2005).
13. Pasterkamp, R.J. *et al.* Expression of the gene encoding the chemorepellent semaphorin III is induced in the fibroblast component of neural scar tissue formed following injuries of adult but not neonatal CNS. *Mol. Cell. Neurosci.* **13**, 143–166 (1999).
14. Pasterkamp, R.J., Anderson, P.N. & Verhaagen, J. Peripheral nerve injury fails to induce growth of lesioned ascending column axons into spinal cord scar tissue expressing the axon repellent Semaphorin3A. *Eur. J. Neurosci.* **13**, 457–471 (2001).
15. Bradbury, E.J. *et al.* Chondroitinase ABC promotes functional recovery after spinal cord injury. *Nature* **416**, 636–640 (2002).
16. De Winter, F. *et al.* Injury-induced class 3 semaphorin expression in the rat spinal cord. *Exp. Neurol.* **175**, 61–75 (2002).
17. Morgenstern, D.A., Asher, R.A. & Fawcett, J.W. Chondroitin sulphate proteoglycans in the CNS injury response. *Prog. Brain Res.* **137**, 313–332 (2002).
18. Silver, J. & Miller, J.H. Regeneration beyond the glial scar. *Nat. Rev. Neurosci.* **5**, 146–156 (2004).
19. Kolodkin, A.L., Matthes, D.J. & Goodman, C.S. The semaphorin genes encode a family of transmembrane and secreted growth cone guidance molecules. *Cell* **75**, 1389–1399 (1993).
20. Luo, Y., Raible, D. & Raper, J.A. Collapsin: a protein in brain that induces the collapse and paralysis of neuronal growth cones. *Cell* **75**, 217–227 (1993).
21. Goshima, Y., Nakamura, F., Strittmatter, P. & Strittmatter, S.M. Collapsin-induced growth cone collapse mediated by an intracellular protein related to *unc-33*. *Nature* **376**, 509–514 (1995).
22. Taniguchi, M. *et al.* Disruption of semaphorin III/D gene causes severe abnormality in peripheral nerve projection. *Neuron* **19**, 519–530 (1997).
23. Sasaki, Y. *et al.* Fyn and Cdk5 mediate semaphorin-3A signaling which is involved in regulation of dendrite orientation in cerebral cortex. *Neuron* **35**, 907–920 (2002).
24. Uchida, Y. *et al.* Semaphorin-3A signaling is mediated via sequential Cdk5 and GSK3b phosphorylation of CRMP2: implication of common phosphorylating mechanism underlying axon guidance and Alzheimer's disease. *Genes Cells* **10**, 165–179 (2005).
25. Kikuchi, K. *et al. In vitro* and *in vivo* characterization of a novel Semaphorin 3A inhibitor, SM-216289 or xanthofulvin. *J. Biol. Chem.* **278**, 42985–42991 (2003).
26. Kumagai, K., Hosotani, N., Kikuchi, K., Kimura, T. & Saji, I. Xanthofulvin, a novel semaphorin inhibitor produced by a strain of *Penicillium*. *J. Antibiot.* **56**, 610–616 (2003).
27. He, Z. & Tessier-Lavigne, M. Neuropilin is a receptor for the axonal chemorepellent semaphorin III. *Cell* **90**, 739–751 (1997).
28. Kitsukawa, T. *et al.* Neuropilin-semaphorin III/D-mediated chemorepulsive signals play a crucial role in peripheral nerve projection in mice. *Neuron* **19**, 995–1005 (1997).
29. Kolodkin, A.L. *et al.* Neuropilin is a Semaphorin III receptor. *Cell* **90**, 753–762 (1997).
30. Takahashi, T. *et al.* Plexin-neuropilin-1 complexes form functional semaphorin-3A receptors. *Cell* **99**, 59–69 (1999).
31. Tamagnone, L. *et al.* Plexins are a large family of receptors for transmembrane, secreted, and GPI-anchored semaphorins in vertebrates. *Cell* **99**, 71–80 (1999).
32. Yaron, A., Huang, P.H., Cheng, H.J. & Tessier-Lavigne, M. Differential requirement for Plexin-A3 and -A4 in mediating responses of sensory and sympathetic neurons to distinct class 3 Semaphorins. *Neuron* **45**, 513–523 (2005).
33. Christensen, M.D. & Hulsebosch, C.E. Spinal cord injury and anti-NGF treatment results in changes in CGRP density and distribution in the dorsal horn in the rat. *Exp. Neurol.* **147**, 463–475 (1997).
34. Romero, M.I. *et al.* Extensive sprouting of sensory afferents and hyperalgesia induced by conditional expression of nerve growth factor in the adult spinal cord. *J. Neurosci.* **20**, 4435–4445 (2000).
35. Romero, M.I., Rangappa, N., Garry, M.G. & Smith, G.M. Functional regeneration of chronically injured sensory afferents into adult spinal cord after neurotrophin gene therapy. *J. Neurosci.* **21**, 8408–8416 (2001).
36. Bregman, B.S. Spinal cord transplants permit the growth of serotonergic axons across the site of neonatal spinal cord transection. *Brain Res.* **431**, 265–279 (1987).
37. Eickholt, B.J., Mackenzie, S.L., Graham, A., Walsh, F.S. & Doherty, P. Evidence for collapsin-1 functioning in the control of neural crest migration in both trunk and hindbrain regions. *Development* **126**, 2181–2189 (1999).
38. Bagnard, D. *et al.* Semaphorin 3A-vascular endothelial growth factor-165 balance mediates migration and apoptosis of neural progenitor cells by the recruitment of shared receptor. *J. Neurosci.* **21**, 3332–3341 (2001).
39. Bagri, A. & Tessier-Lavigne, M. Neuropilins as Semaphorin receptors: *in vivo* functions in neuronal cell migration and axon guidance. *Adv. Exp. Med. Biol.* **515**, 13–31 (2002).
40. Archelos, J.J. *et al.* Production and characterization of monoclonal antibodies to the extracellular domain of P0. *J. Neurosci. Res.* **35**, 46–53 (1993).
41. Basso, D.M., Beattie, M.S. & Bresnahan, J.C. A sensitive and reliable locomotor rating scale for open field testing in rats. *J. Neurotrauma* **12**, 1–21 (1995).
42. Mikami, Y. *et al.* A simple and reliable behavioral analysis of locomotor function after spinal cord injury in mice. Technical note. *J. Neurosurg.* **97**, 142–147 (2002).
43. Bareyre, F.M. *et al.* The injured spinal cord spontaneously forms a new intraspinal circuit in adult rats. *Nat. Neurosci.* **7**, 269–277 (2004).
44. Morrison, S.J., White, P.M., Zock, C. & Anderson, D.J. Prospective identification, isolation by flow cytometry, and *in vivo* self-renewal of multipotent mammalian neural crest stem cells. *Cell* **96**, 737–749 (1999).
45. Cai, D., Shen, Y., De Bellard, M., Tang, S. & Filbin, M.T. Prior exposure to neurotrophins blocks inhibition of axonal regeneration by MAG and myelin via a cAMP-dependent mechanism. *Neuron* **22**, 89–101 (1999).
46. McTigue, D.M., Horner, P.J., Stokes, B.T. & Gage, F.H. Neurotrophin-3 and brain-derived neurotrophic factor induce oligodendrocyte proliferation and myelination of regenerating axons in the contused adult rat spinal cord. *J. Neurosci.* **18**, 5354–5365 (1998).
47. Ikegami, T. *et al.* Chondroitinase ABC combined with neural stem/progenitor cell transplantation enhances graft cell migration and outgrowth of growth-associated protein-43-positive fibers after rat spinal cord injury. *Eur. J. Neurosci.* **22**, 3036–3046 (2005).
48. Okada, S. *et al.* Conditional ablation of Stat3 or Socs3 discloses a dual role for reactive astrocytes after spinal cord injury. *Nat. Med.* **12**, 829–834 (2006).
49. Guthrie, S. & Lumsden, A. Collagen gel coculture of neural tissue. *Neuroprotocols* **4**, 116–120 (1994).
50. Thomaidou, D. *et al.* Soluble forms of NCAM and F3 neuronal cell adhesion molecules promote Schwann cell migration: identification of protein tyrosine phosphatases zeta/beta as the putative F3 receptors on Schwann cells. *J. Neurochem.* **78**, 767–778 (2001).

Available online at www.sciencedirect.com
SCIENCE DIRECT®
Neuroscience Research 54 (2006) 11–14
Neuroscience Research
www.elsevier.com/locate/neures

Underediting of GluR2 mRNA, a neuronal death inducing molecular change in sporadic ALS, does not occur in motor neurons in ALS1 or SBMA

Yukio Kawahara [a,1], Hui Sun [a], Kyoko Ito [a], Takuto Hideyama [a], Masashi Aoki [b], Gen Sobue [c], Shoji Tsuji [a], Shin Kwak [a,*]

[a] *Department of Neurology, Graduate School of Medicine, The University of Tokyo, 7-3-1 Hongo, Bunkyo-ku, Tokyo 113-8655, Japan*
[b] *Department of Neurology, Tohoku University Graduate School of Medicine, Sendai, Japan*
[c] *Department of Neurology, Nagoya University Graduate School of Medicine, Nagoya, Japan*

Received 7 July 2005; accepted 13 September 2005
Available online 12 October 2005

Abstract

Deficient RNA editing of the AMPA receptor subunit GluR2 at the Q/R site is a primary cause of neuronal death and recently has been reported to be a tightly linked etiological cause of motor neuron death in sporadic amyotrophic lateral sclerosis (ALS). We quantified the RNA editing efficiency of the GluR2 Q/R site in single motor neurons of rats transgenic for mutant human Cu/Zn-superoxide dismutase (SOD1) as well as patients with spinal and bulbar muscular atrophy (SBMA), and found that GluR2 mRNA was completely edited in all the motor neurons examined. It seems likely that the death cascade is different among the dying motor neurons in sporadic ALS, familial ALS with mutant SOD1 and SBMA.

Keywords: ALS; SOD1; Spinal and bulbar muscular atrophy; Motor neuron; RNA editing; GluR2; AMPA receptor; Neuronal death

1. Introduction

Amyotrophic lateral sclerosis (ALS) is a progressive neurodegenerative disease with selective loss of both upper and lower motor neurons, and familial cases are rare. The etiology of sporadic ALS remains elusive but recently deficient RNA editing of AMPA receptor subunit GluR2 at the Q/R site is reported in motor neurons in ALS that occurs in a disease-specific and motor neuron-selective manner (Kawahara et al., 2004; Kwak and Kawahara, 2005). Moreover, underediting of the GluR2 Q/R site greatly increases the Ca^{2+} permeability of AMPA receptors (Hume et al., 1991; Verdoorn et al., 1991; Burnashev et al., 1992), which may cause neuronal death due to increased Ca^{2+} influx through the receptor channel, hence mice with RNA editing deficiencies at the GluR2 Q/R site die young (Brusa et al., 1995) and mice transgenic for an artificial Ca^{2+}-permeable GluR2 develop motor neuron disease 12 months after birth (Kuner et al., 2005). Such evidence lends strong support to the close relevance of deficient RNA editing of the GluR2 at the Q/R site to death of motor neurons in sporadic ALS. However, although we and other researchers have demonstrated that dying neurons in several neurodegenerative diseases exhibit edited GluR2 (Kwak and Kawahara, 2005), it has not yet been demonstrated whether the underediting of GluR2 occurs in dying motor neurons in motor neuron diseases other than ALS. Such investigation is of particular importance since it will help clarify whether the molecular mechanism of motor neurons death is common among various subtypes of motor neurons.

ALS associated with the SOD1 mutation (ALS1) is the most frequent familial ALS (Rosen et al., 1993), and mutated human SOD1 transgenic animals have been studied extensively as a disease model of ALS1, yet the etiology of neuronal death in the animals has not been elucidated. Another example of non-ALS motor neuron disease is spinal and bulbar muscular atrophy (SBMA), which predominantly affects lower motor neurons with a relatively slow clinical course. Since the CAG

* Corresponding author. Tel.: +81 3 5800 8672; fax: +81 3 5800 6548.
E-mail address: kwak-tky@umin.ac.jp (S. Kwak).
[1] Present address: The Wistar Institute, Philadelphia, PA, USA.

0168-0102/$ – see front matter
doi:10.1016/j.neures.2005.09.006

Table 1
RNA editing efficiency of single motor neurons in SBMA

Case	Age at death (year)	Sex	No. of CAG repeats[a]	Postmortem delay (h)	GluR2(+) MN[b]	MN with 100% editing efficiency (% of GluR2(+) MN)
SBMA, case 1	71	M	48	2.5	12	12 (100)
SBMA, case 2	78	M	42	2.5	16	16 (100)
SBMA, case 3	60	M	44	1	16	16 (100)

[a] Number of CAG repeats in the androgen receptor gene.
[b] Motor neurons in which GluR2 RT-PCR amplifying product was detected.

repeat expansion in the androgen receptor gene has been demonstrated in SBMA (La Spada et al., 1991), and pharmacological castration is therapeutically effective in animal models (Katsuno et al., 2002, 2003), the death cascade responsible for SBMA is likely different from sporadic ALS. In this paper, an investigation is carried out into whether or not the dying mechanism underlying sporadic ALS is the same as ALS1 and SBMA by determining the editing status of the GluR2 Q/R site in single motor neurons.

2. Materials and methods

The animals used in this study were SOD1^{G93A} and SOD1^{H46R} transgenic male rats (Nagai et al., 2001) ($n = 3$ each) that had exhibited progressive neuromuscular weakness with their littermates as the control ($n = 3$ each) (Table 2). The first sign of disease in these rats was weakness of their hindlimbs, mostly exhibited by the dragging of one limb. Onset of motor neuron disease was scored as the first observation of abnormal gait or evidence of limb weakness. The mean age of onset of clinical weakness for the SOD1^{G93A} and SOD1^{H46R} lines was 122.9 ± 14.1 and 144.7 ± 6.4 days, respectively. As the disease progressed, the rats exhibited marked muscle wasting in their hindlimbs, and then in the forelimbs. The mean duration after the clinical expression of the disease in the SOD1^{G93A} and SOD1^{H46R} lines was 8.3 ± 0.7 and 24.2 ± 2.9 days, respectively (Nagai et al., 2001). The rats were killed 3 days and 2 weeks after the onset for the SOD1^{G93A} and SOD1^{H46R} lines, respectively, and we examined their fifth lumbar cord. Animals were handled according to Institutional Animal Care and Use Committee approved protocols that are in line with the Guideline for Animal Care and Use by the National Institute of Health. Spinal cords were isolated after deep pentobarbiturate anesthesia. In addition, spinal cords were obtained at autopsy from three genetically confirmed patients with SBMA (Table 1). Written informed consent was obtained from all subjects prior to death or from their relatives, and the Ethics Committees of Graduate School of Medicine, the University of Nagoya and the University of Tokyo approved the experimental procedures used. Spinal cords were rapidly frozen on dry ice and maintained at −80 °C until use.

Table 2
RNA editing efficiency of single motor neurons in mutated human SOD1 transgenic rats

Case (n)	GluR2(+) MN[a]	MN with 100% editing efficiency (% of GluR2(+) MN)
SOD1^{G93A}-1	13	13 (100)
SOD1^{G93A}-2	21	21 (100)
SOD1^{G93A}-3	21	21 (100)
SOD1^{H46R}-1	19	19 (100)
SOD1^{H46R}-2	23	23 (100)
SOD1^{H46R}-3	20	20 (100)
SOD1^{G93A}, littermates (3)	22	22 (100)
SOD1^{H46R}, littermates (3)	20	20 (100)

[a] Motor neurons in which GluR2 RT-PCR amplifying product was detected.

Single motor neurons were isolated and collected into respective single test tubes that contained 200 μl of TRIZOL Reagent (Invitrogen Corp., Carlsbad, CA, USA) using a laser microdissection system as previously described (Kawahara et al., 2003b, 2004) (LMD, Leica Microsystems Ltd., Germany) (Fig. 1a). After extracting total RNA from single neuron tissue, we analyzed the RNA editing efficiency at the GluR2 Q/R site by means of RT-PCR coupled with digestion of the PCR amplified products with a restriction enzyme Bbv-1 (New England BioLabs, Beverly, MA, USA) (Takuma et al., 1999; Kawahara et al., 2003a, 2004), and the editing efficiency was calculated by quantitatively analyzing the digests with a 2100 Bioanalyser (Agilent Technologies, Palo Alto, CA, USA), as previously described (Kawahara et al., 2003a). Briefly, after gel purification using Zymoclean Gel DNA Recovery Kit according to the manufacturer's protocol (Zymo Research, Orange, CA, USA), PCR products were quantified using a 2100 Bioanalyser. An aliquot (0.5 μg) was then incubated at 37 °C for 12 h with 10 × restriction buffer and 2 U of *Bbv*I in a total volume of 20 μl and inactivated at 65 °C for 30 min. The PCR products had one intrinsic *Bbv*I recognition sites, whereas the products originating from unedited GluR2 mRNA had an additional recognition site. Thus, restriction digestion of the PCR products originating from edited rat (278 bp) and human (182 bp) GluR2 mRNA should produce two bands (human GluR2 in parenthesis) at 219 (116) and 59 (66) bp, whereas those originating from unedited GluR2 mRNA should produce three bands at 140 (81), 79 (35), and 59 (66) bp. As the 59 (66) bp band would originate from both edited and unedited mRNA, but the 219 (116) bp band would originate from only edited mRNA, we quantified the molarity of the 219 (116) and 59 (66) bp bands using the 2100 Bioanalyser and calculated the editing efficiency as the ratio of the former to the latter for each sample.

The following primers were used for PCR for rat and human GluR2 (amplified product lengths are also indicated): for rat GluR2 (278 bp): rF (5′-AGCAGATTTAGCCCCTACGAG-3′) and rR (5′-CAGCACTTTCGATGGGAGACAC-3′). for human GluR2, the first PCR (187 bp): hG2F1 (5′-TCTGGTTTTCCTTGGGTGCC-3′) and hG2R1 (5′-AGATCCTCAGCACTTTCG-3′); for the nested PCR (182 bp): hG2F2 (5′-GGTTTTCCTTGGGTGCCTTTAT-3′) and hG2R2 (5′-ATCCTCAGCACTTTCGATGG-3′). We confirmed that these primer pairs were situated in two distinct exons with an intron between them and did not amplify products originating from other GluR subunits (data not shown). PCR amplification for rat GluR2 was initiated with a denaturation step that was carried out at 95 °C for 2 min, followed by 40 cycles of 95 °C for 30 s, 62 °C for 30 s, and 72 °C for 1 min. PCR amplification for human GluR2 began with a 1 min denaturation step at 95 °C, followed by 35 cycles of denaturation at 95 °C for 10 s, annealing at 64 °C for 30 s and extension at 68 °C for 60 s. Nested PCR was conducted on 2 μl of the first PCR product under the same conditions with the exception of the annealing temperature (66 °C).

3. Results

The number of motor neurons was severely decreased in the spinal cord of SBMA patients, and we analyzed 44 neurons dissected from three cases (12 from case 1, 16 from cases 2 and 3). Restriction digestion of the PCR products yielded only 116 and 66 bp fragments but no 81 or 35 bp fragments as seen in ALS motor neurons in all the SBMA motor neurons examined. Likewise, restriction digestion of the PCR products from motor

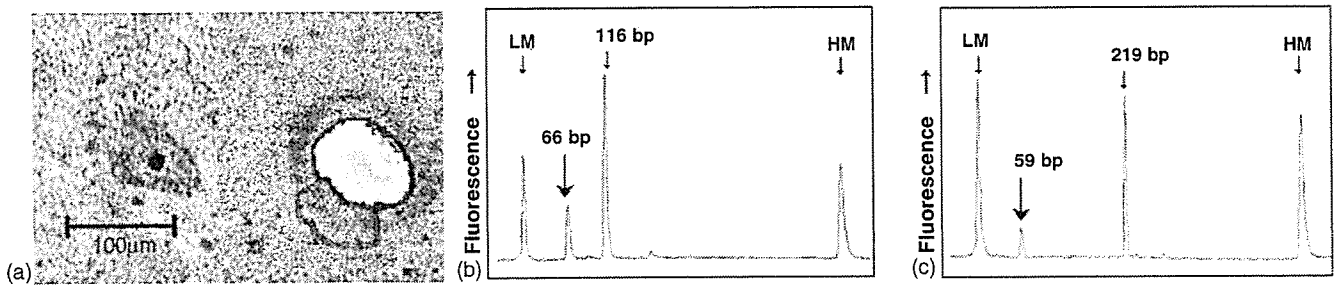

Fig. 1. (a) A single motor neuron from an SBMA patient before (left) and after (right) the dissection with a laser-microdissector. (b and c) An example of electropherogram by a 2100 Bioanalyser. Samples are the Bbv-1-digest of PCR product from tissues of a single motor neuron from an SBMA patient (b) and from a mutated human $SOD1^{G93A}$ transgenic mouse (c). LM: lower marker (15 bp), HM: higher marker (600 bp).

neurons of mutated human SOD1 transgenic rats yielded only 219 and 59 bp fragments (Fig. 1). Therefore, the values of RNA editing efficiency at the Q/R site of GluR2 were 100% in 44 motor neurons from three SBMA cases (Table 1), 55 single motor neurons from three $SOD1^{G93A}$ transgenic rats, 62 neurons from three $SOD1^{H46R}$ transgenic rats, as well as in 42 neurons from three littermate rats of each group (Table 2). The consistent finding that the GluR2 Q/R site is 100% edited in motor neurons of SBMA patients and transgenic rats for mutated human SOD1 is in marked contrast to the finding in ALS motor neurons that the editing efficiency widely varied among neurons ranging from 0% to 100% (Kawahara et al., 2004).

4. Discussion

Compared to the significant underediting reported for the GluR2 Q/R site in motor neurons of sporadic ALS (Kawahara et al., 2004), GluR2 mRNA in all the examined motor neurons of the mutated human SOD1 transgenic rats with two different mutation sites and SBMA patients was completely edited at the Q/R site. We have confirmed that postmortem delay hardly influenced the editing efficiency at the GluR2 Q/R site (Kawahara et al., 2003b), hence the significant difference in the postmortem delay between the SBMA patients in this study and ALS patients in the previous report (Kawahara et al., 2004) would not have affected these results. We examined the motor neurons in the spinal cord segment corresponding to the hindlimb of mutated human SOD1 transgenic rats after their hindlimbs had become weak, indicating that the motor neurons examined were already pathologically affected. Likewise, we found that only a small number of motor neurons remained in the spinal cord of SBMA patients. Thus our results indicate that GluR2 RNA editing was complete in the dying motor neurons in both the mutated human SOD1 transgenic rats and SBMA patients, implying that the neuronal death mechanism is not due to the underediting of GluR2 mRNA seen in sporadic ALS. Since the pathogenic mechanism underlying ALS1 is considered to be the same as in mutant human SOD1 transgenic animals, motor neurons in affected ALS1 patients would be expected to have only edited GluR2 mRNA. Indeed, an association study of the SOD1 gene in a considerable number of patients with sporadic ALS reported no significant association with mutations of the SOD1 gene (Jackson et al., 1997). Due to the lack of appropriate animal model for sporadic ALS, mutant human SOD1 transgenic animals have been used as a model for ALS in general, particularly in studies searching for therapeutically effective drugs. However, it should be kept in mind that mutated human SOD1 transgenic animals are merely a suggestive model for sporadic ALS and a gain of toxic function in mutated SOD1 kills motor neurons via mechanisms other than the demise of RNA editing. There are likely multiple different death pathways in motor neurons, and motor neurons in sporadic ALS, ALS1 and SBMA die by different death cascades.

Acknowledgements

This investigation was supported in part by grants-in-aid for Scientific Research on Priority Areas from the Ministry of Education, Culture, Sports, Science and Technology of Japan and grants from the Ministry of Health, Labor and Welfare of Japan (to SK), and a grant from Japan ALS Association (to YK).

References

Brusa, R., Zimmermann, F., Koh, D., Feldmeyer, D., Gass, P., Seeburg, P., Sprengel, R., 1995. Early-onset epilepsy and postnatal lethality associated with an editing-deficient GluR-B allele in mice. Science 270, 1677–1680.

Burnashev, N., Monyer, H., Seeburg, P., Sakmann, B., 1992. Divalent ion permeability of AMPA receptor channels is dominated by the edited form of a single subunit. Neuron 8, 189–198.

Hume, R.I., Dingledine, R., Heinemann, S.F., 1991. Identification of a site in glutamate receptor subunits that controls calcium permeability. Science 253, 1028–1031.

Jackson, M., Al-Chalabi, A., Enayat, Z.E., Chioza, B., Leigh, P.N., Morrison, K.E., 1997. Copper/zinc superoxide dismutase 1 and sporadic amyotrophic lateral sclerosis: analysis of 155 cases and identification of a novel insertion mutation. Ann. Neurol. 42, 803–807.

Katsuno, M., Adachi, H., Doyu, M., Minamiyama, M., Sang, C., Kobayashi, Y., Inukai, A., Sobue, G., 2003. Leuprorelin rescues polyglutamine-dependent phenotypes in a transgenic mouse model of spinal and bulbar muscular atrophy. Nat. Med. 9, 768–773.

Katsuno, M., Adachi, H., Kume, A., Li, M., Nakagomi, Y., Niwa, H., Sang, C., Kobayashi, Y., Doyu, M., Sobue, G., 2002. Testosterone reduction prevents phenotypic expression in a transgenic mouse model of spinal and bulbar muscular atrophy. Neuron 35, 843–854.

Kawahara, Y., Ito, K., Sun, H., Aizawa, H., Kanazawa, I., Kwak, S., 2004. RNA editing and death of motor neurons. Nature 427, 801.

Kawahara, Y., Ito, K., Sun, H., Kanazawa, I., Kwak, S., 2003a. Low editing efficiency of GluR2 mRNA is associated with a low relative abundance of

ADAR2 mRNA in white matter of normal human brain. Eur. J. Neurosci. 18, 23–33.

Kawahara, Y., Kwak, S., Sun, H., Ito, K., Hashida, H., Aizawa, H., Jeong, S.-Y., Kanazawa, I., 2003b. Human spinal motoneurons express low relative abundance of GluR2 mRNA: an implication for excitotoxicity in ALS. J. Neurochem. 85, 680–689.

Kuner, R., Groom, A.J., Bresink, I., Kornau, H.C., Stefovska, V., Muller, G., Hartmann, B., Tschauner, K., Waibel, S., Ludolph, A.C., Ikonomidou, C., Seeburg, P.H., Turski, L., 2005. Late-onset motoneuron disease caused by a functionally modified AMPA receptor subunit. Proc. Natl. Acad. Sci. U.S.A. 102, 5826–5831.

Kwak, S., Kawahara, Y., 2005. Deficient RNA editing of GluR2 and neuronal death in amyotropic lateral sclerosis. J. Mol. Med. 83, 110–120.

La Spada, A.R., Wilson, E.M., Lubahn, D.B., Harding, A.E., Fischbeck, K.H., 1991. Androgen receptor gene mutations in X-linked spinal and bulbar muscular atrophy. Nature 352, 77–79.

Nagai, M., Aoki, M., Miyoshi, I., Kato, M., Pasinelli, P., Kasai, N., Brown Jr., R.H., Itoyama, Y., 2001. Rats expressing human cytosolic copper–zinc superoxide dismutase transgenes with amyotrophic lateral sclerosis: associated mutations develop motor neuron disease. J. Neurosci. 21, 9246–9254.

Rosen, D.R., Siddique, T., Patterson, D., Figlewicz, D.A., Sapp, P., Hentati, A., Donaldson, D., Goto, J., O'Regan, J.P., Deng, H.X., et al., 1993. Mutations in Cu/Zn superoxide dismutase gene are associated with familial amyotrophic lateral sclerosis. Nature 362, 59–62.

Takuma, H., Kwak, S., Yoshizawa, T., Kanazawa, I., 1999. Reduction of GluR2 RNA editing, a molecular change that increases calcium influx through AMPA receptors, selective in the spinal ventral gray of patients with amyotrophic lateral sclerosis. Ann. Neurol. 46, 806–815.

Verdoorn, T., Burnashev, N., Monye, R.H., Seeburg, P., Sakmann, B., 1991. Structural determinants of ion flow through recombinant glutamate receptor channels. Science 252, 1715–1718.

Journal of Neurochemistry, 2006, **98**, 782–791 doi:10.1111/j.1471-4159.2006.03903.x

Slow and selective death of spinal motor neurons *in vivo* by intrathecal infusion of kainic acid: implications for AMPA receptor-mediated excitotoxicity in ALS

Hui Sun,*[,1] Yukio Kawahara,*[,2] Kyoko Ito,* Ichiro Kanazawa† and Shin Kwak*

**Department of Neurology, Graduate School of Medicine, The University of Tokyo, Tokyo, Japan*

†National Center of Neurology and Psychiatry, SORST Japan Science and Technology Corporation, Tokyo, Japan

Abstract

Excitotoxicity mediated by α-amino-3-hydroxy-5-methyl-4-isoxazole propionic acid (AMPA) receptors has been proposed to play a major role in the selective death of motor neurons in sporadic amyotrophic lateral sclerosis (ALS), and motor neurons are more vulnerable to AMPA receptor-mediated excitotoxicity than are other neuronal subclasses. On the basis of the above evidence, we aimed to develop a rat model of ALS by the long-term activation of AMPA receptors through continuous infusion of kainic acid (KA), an AMPA receptor agonist, into the spinal subarachnoid space. These rats displayed a progressive motor-selective behavioral deficit with delayed loss of spinal motor neurons, mimicking the clinicopathological characteristics of ALS. These changes were significantly ameliorated by co-infusion with 6-nitro-7-sulfamobenso(f)quinoxaline-2,3-dione (NBQX), but not with D(−)-2-amino-5-phosphonovaleric acid (APV), and were exacerbated by co-infusion with cyclothiazide, indicative of an AMPA receptor-mediated mechanism. Among the four AMPA receptor subunits, expression of GluR3 mRNA was selectively up-regulated in motor neurons but not in dorsal horn neurons of the KA-infused rats. The up-regulation of GluR3 mRNA in this model may cause a molecular change that induces the selective vulnerability of motor neurons to KA by increasing the proportion of GluR2-lacking (i.e. calcium-permeable) AMPA receptors. This rat model may be useful in investigating ALS etiology.

Keywords: amyotrophic lateral sclerosis, AMPA receptor, excitotoxicity, GluR3, GluR2, RNA editing.

J. Neurochem. (2006) **98**, 782–791.

The most common motor neuron disease, amyotrophic lateral sclerosis (ALS), is a progressive neurodegenerative disease characterized by selective upper and lower motor neuron loss that is initiated in mid-life and leads to death as a result of respiratory muscular weakness. ALS has a uniform worldwide prevalence (five cases per 100 000 individuals), of which sporadic ALS accounts for more than 90% of all cases and only the remaining 5% of cases are familial (FALS) (Roland *et al.* 2005). Despite the fact that a good animal model is indispensable for investigating the etiology and for developing novel therapies for a disease, few appropriate animal models for sporadic ALS have been developed. Among the animal models tested, animal lines transgenic for the mutated human *Cu/Zn superoxide dismutase* (*SOD1*) gene (Gurney *et al.* 1994; Nagai *et al.* 2001; Howland *et al.* 2002) are regarded as a candidate disease model for all types of ALS, but the etiology of the FALS caused by the *SOD1* gene mutation is not necessarily the same as that of sporadic ALS. Indeed, the extent of neuropathological changes is not confined to motor neurons in these animals (Gurney *et al.* 1994), and although *SOD1* gene mutations have been found in a small population of patients with sporadic ALS, no significant association has been detected between sequence variants in the SOD1 locus and sporadic ALS

Received January 6, 2006; revised manuscript received March 15, 2006; accepted March 20, 2006.

Address correspondence and reprint requests to Shin Kwak MD PhD, Department of Neurology, Graduate School of Medicine, The University of Tokyo, 7-3-1 Hongo, Bunkyo-ku, Tokyo 113–8655, Japan.
E-mail: kwak-tky@umin.ac.jp

[1]Present address: National Institute for Longevity Sciences, Obu, Japan.
[2]Present address: the Wistar Institute, Philadelphia, PA, USA.

Abbreviations used: aCSF, artificial cerebrospinal fluid; ALS, amyotrophic lateral sclerosis; AMPA, α-amino-3-hydroxy-5-methyl-4-isoxazole propionic acid; APV, D(−)-2-amino-5-phosphonovaleric acid; CTZ, cyclothiazide; F, Fischer; FALS, familial ALS; KA, kainic acid; NBQX, 6-nitro-7-sulfamobenso(f)quinoxaline-2,3-dione; PBS, phosphate-buffered saline; SOD1, Cu/Zn superoxide dismutase; W, Wistar.

